JET-P(93)61

An Assessment of Theoretical Models based on Observations in the JET Tokamak

Part II: Heat Transport due to Electron Drift Waves, Electro-Magnetic and Resistive Fluid Turbulence, and Magnetic Islands

F Tibone, J W Connor[1], T E Stringer, H R Wilson[1].

JET Joint Undertaking, Abingdon, Oxon, OX14 3EA, UK.
[1] AEA Technology, Fusion, Culham, Abingdon, OX14 3DB, UK.
(Euratom/UKAEA Fusion Association)

Preprint of a paper to be submitted for publication in
Plasma Physics and Controlled Nuclear Fusion.

August 1993

ABSTRACT

Theoretical estimates of the electron thermal diffusivity, driven by different instabilities to which tokamak plasmas are prone, are surveyed and their regions of validity specified. For those that are applicable, the prediction for a typical set of JET profiles is compared with the experimental local diffusivity. The predicted and experimental scalings of the thermal diffusivity with key parameters are also compared. Although no one model reproduces the magnitude, radial variation, and parameter scalings of the experimental thermal diffusivity, several models correctly predict some of the experimental behaviour.

1. INTRODUCTION

In a companion paper (CONNOR et al. (1993)) we have reviewed theoretical models for anomalous ion energy transport due to ion temperature gradient instabilities, and compared their predictions with the experimental plasma behaviour as observed in JET. Here we discuss results of a similar investigation carried out for models of electron energy transport. The objective is to identify theories that are compatible with data inferred from JET measurements, and may therefore be relevant to the understanding of energy transport in tokamaks. This work should be regarded as a first step towards an exhaustive assessment of such theories, which will require detailed simulations of the observed plasma behaviour in various regions of parameter space.

As in CONNOR et al. (1993), for each theory we will first examine the assumptions made in the original derivation and the applicability to plasma conditions obtained in JET. For those models that are applicable, the expected transport coefficients or heat fluxes will then be compared with those inferred from experimental observations.

The assessment is made in terms of local parameters, using the results of power balance analyses of JET plasmas based on measurements of density, temperature, etc. which are resolved both spatially and in time. The techniques adopted for the local transport analysis, together with the inherent uncertainties and the main observed trends, are discussed in detail in Section 2 of CONNOR et al. (1993). Here we shall only mention that the experimental determination of the specific electron (as opposed to total) heat transport properties is possible in practice only for a limited set of JET plasmas. Therefore one generally has to refer to observed local transport for the plasma regarded as a single fluid; the experimental quantity used here for the comparisons with theory is an "effective" thermal conductivity defined as $\chi_{eff}^{EXP} \equiv -(q_e + q_i)_{cond} / (2n_e\nabla T_e)$, which corresponds to an assumption of equal ion and electron heat losses (q_j being here the local heat flux for species j).

Since losses through the ion channel are often dominant in JET plasmas, as discussed in CONNOR et al. (1993), χ_{eff}^{EXP} should be regarded as an upper bound on the actual electron thermal conductivity, which will however be of the same order of magnitude. The parametric dependences of the "true" χ_e need of course not be exactly the same as those of χ_{eff}^{EXP}, since χ_i and χ_e may scale differently. We shall however assume that a good theoretical model for χ_e ought to predict scalings that are not opposite to those observed for χ_{eff}^{EXP}.

The theories assessed in this paper consider different instabilities as possible causes for anomalous transport. Models based on drift wave turbulence, electromagnetic fluctuations, resistive fluid turbulence and magnetic islands will be examined in Sections 2, 3, 4 and 5 respectively. The "critical electron temperature gradient" model has been compared with JET data in depth elsewhere (REBUT et al. (1991)) and will not be discussed here. A discussion of the overall results, and conclusions, will be given in Section 6.

Definitions of all non-standard symbols used in this paper are given in the Appendix.

2. ELECTRON DRIFT WAVE TRANSPORT

In this section we consider the electron drift wave with a frequency $\omega \sim \omega_{*e}$, where $\omega_{*e} \sim k_\perp \rho_s c_s / L_n$ is the electron drift frequency, which provides a possible mechanism for the anomalous electron energy transport. The simplest description of the electron drift wave is in slab geometry, where it is found that, to overcome the damping effect of the magnetic shear, it is necessary to consider a nonlinear theory. Such an analysis is discussed in the next subsection. We then consider the effects of introducing toroidal geometry. One then finds that toroidicity tends to reduce the shear damping and thus drive the mode more unstable. Toroidal geometry also introduces trapped particles and in the third subsection we consider instabilities that are induced by a trapped electron population. These modes have been studied extensively in the literature using a variety of models, so we find it convenient to categorise these trapped electron modes according to the method of analysis. We then consider the effects of inverted density profiles and finally look at a trapped electron mode which has been derived in the limit of short perpendicular wavelength.

2.1 Circulating Electron Drift Wave in a Slab/Cylinder

The collisionless electron drift wave gives rise to a mode (the 'universal mode') which, in slab or cylindrical geometry, is always unstable in the absence of (magnetic) shear. When shear is present the mode is found to be stable (ROSS and MAHAJAN (1978), TSANG et al. (1978)) as a result of 'radiative' or shear damping (PEARLSTEIN and BERK (1969)).

However, HIRSHMAN and MOLVIG (1979) consider the effects of electrostatic turbulence on the mode. They argue that the effect of stochastic diffusion of the electron orbits due to this turbulence will be such as to destabilise the mode. The nonlinear effects are studied through an **E x B** term in the drift equation. From this a 'nonlinear' dispersion relation is derived which demonstrates that quite low levels of turbulence (typically below those expected to exist in tokamaks) are required to drive the mode unstable. Solving the dispersion relation at marginal stability (i.e. when the driving of the mode due to the action of the turbulence on the electrons is balanced by shear damping) then determines the diffusion coefficient D and

$$\chi_e \sim \frac{3D}{2} = \frac{45}{2} \Delta_{PB}^{3/2} \tau^{5/2} \left[\frac{1+\tau}{2}\right]^{-9/2} \frac{c_s \rho_s^2}{L_s} \tag{1}$$

with

$$\Delta_{PB} = \left(\frac{L_s}{L_n}\right)^3 \left(\frac{m_e}{m_i}\right) \tag{2}$$

In a subsequent paper, MOLVIG et al. (1979) investigate the effects of turbulence on the electro-magnetic electron drift wave in slab geometry. Using similar techniques to those employed in their electrostatic theory, they find that the electro-magnetic version is important when the ratio of electron thermal pressure to the magnetic pressure, β_e, exceeds the electron-ion mass ratio, i.e. $\beta_e > (m_e/m_i)$ ($\beta_e = 2\mu_o p_e/B^2$, where the units are SI). This condition is usually satisfied in JET plasmas, except in the proximity of the outer boundary. The diffusion coefficient is then given by

$$\chi_e \sim D = \frac{0.14}{\tau^{3/2}}\left(\frac{\tau}{1+\tau}\right)^4\left(\frac{m_e}{m_i\beta_e}\right)\left(\frac{L_s}{L_n}\right)^2\frac{c_s\rho_s^2}{L_n} \tag{3}$$

To compare these predictions with the experimentally observed behaviour of JET plasmas, we examine first the magnitude and radial dependence of transport coefficients for one representative set of discharge parameters (Fig. 1a), and then put this in context by showing the effect, at a fixed radial position, of a wide range of variation in the main plasma parameters (Fig. 1b).

Figure 1a shows predicted and observed transport for a typical L-mode JET discharge; the experimental data were described in detail in Section 2 of the companion paper. χ_e^{TH} from the electro-magnetic theory is clearly much too low, while the transport due to electrostatic turbulence accounts for a fraction of the observed χ_{eff}. Interestingly, in spite of their strong temperature dependence, both theoretical predictions increase sharply near the plasma edge, towards realistic values, mostly as a result of the rapid decrease of the density scale length in that region.

Figure 1b, based on a set of data corresponding to sawtooth-free JET plasmas obtained in various operating conditions, shows a similar picture across a wide range of parameter variation. The further decrease of χ_e^{TH} at high density is due mainly to a flattening of the density profile, i.e. it is again a reflection of the strong L_n-dependence.

2.2 Slab-like Drift Wave in a Tokamak

In a slab/cylinder we have seen that stability depends on the competition between electron drive (Landau resonance in the collisionless regime and collisional drive at higher collision frequency) and shear damping and that, in fact, the mode is linearly stable. In a tokamak passing particles continue to provide Landau or collisional drive as appropriate, but shear damping can be cancelled by toroidal effects (TAYLOR (1977)). Thus one can use $D \sim \gamma/k_\perp^2$ estimates of the diffusion where the only contribution to γ is the electron drive (i.e. the shear damping part is dropped). WALTZ et al. (1987) present $\gamma/k_\perp^2$ estimates of the transport due to drift waves. Taking $k_\perp\rho_s \sim 1$ they give the following result for the collisionless diffusion coefficient, which they claim to be applicable in the region $\nu_e/\omega_{te} < 1$:

$$\chi_e \sim D = \frac{c_s\rho_s^2}{L_n}\left(\frac{Rq}{L_n}\right)\left(\frac{m_e}{m_i}\right)^{1/2} \tag{4}$$

Waltz et al. also give an expression which is valid in the collisional regime. This is

$$\chi_e \sim D = \frac{c_s\rho_s^2}{L_n}\left(\frac{Rq}{L_n}\right)\left(\frac{m_e}{m_i}\right)^{1/2}\left(\frac{\nu_e}{\omega_{te}}\right) \tag{5}$$

for $\nu_e/\omega_{te} > 1$. Here, ν_e is the electron collision frequency and $\omega_{te} = v_{te}/(Rq)$ is the electron transit frequency.

Figure 2 shows that in JET plasmas the collisionless expression applies, across the entire cross-section, even in the high density regime; this reflects the high observed electron temperatures. Furthermore these modes are always unstable.

The heat transport predicted by WALTZ et al. (1987) is one order of magnitude less than that observed (Fig. 3); note that this discrepancy would be removed if $k_\perp\rho_s \sim 0.3$ (rather than ~ 1). The dependences on q and L_n in Eq. (4) are sufficient to reverse the unfavourable radial variation which would result from the temperature scaling of the "leading term" in χ_e^{TH}. The remarks made above (Fig. 1b) concerning the density dependence also apply to this model. In addition the q-dependence introduces a favourable scaling of confinement with current, as observed experimentally. This feature was less prominent in Eqs. (1) and (3) because L_s is in practice less sensitive to changes in the plasma current.

2.3 Trapped Electron Induced Modes

In low collisionality machines such as JET, trapped electron effects become important. They provide new mechanisms for destabilising the drift waves. The resulting instabilities are the trapped electron modes (TEMs), which can be sub-divided into dissipative and collisionless modes, depending on whether $\omega_* \lessgtr \nu_{eff}$ where $\nu_{eff} = \nu_e / \varepsilon$ is the effective collision frequency for detrapping the trapped electrons. This section reviews the extensive literature on the transport that might be expected to result from such modes.

Numerous approaches have been developed and the theories have been categorised according to the type of approach that was adopted.

(i) Marginal Stability Approach

This is applied to 'slab-like' trapped particle modes for which shear damping persists. It is based on the assumption that the instability-driven transport is so large that the temperature gradient cannot increase far above marginal stability. In a calculation by MANHEIMER et al. (1976) for the case of the dissipative trapped electron mode, an analytic stability criterion was derived which balances the drive due to collisional detrapping against shear damping appropriate to a slab geometry (a justification for this treatment can be found in CONNOR, TAYLOR and WILSON (1993)). Taking the large aspect ratio limit and assuming $\eta_i = 1$ they derive:

$$4\left(1+\frac{2T_i}{T_e}\right)\frac{L_{T_e}}{L_s\varepsilon^{1/2}} = 1 \qquad (6)$$

as the condition for marginal stability. Instability occurs when the left hand side is less than unity. The neglect of the collisionless electron magnetic drifts requires $\varepsilon_n < 1$.

Figure 4a compares for a single shot the measured temperature scale length with that corresponding to marginal stability. Bearing in mind that uncertainties affect the estimate of both quantities, the core region of maximum temperature gradient ($0.2 \le \rho \le 0.4$) might be interpreted as marginally stable. On the other hand, in the outer region where global confinement is mostly determined, the plasma appears to be stable. This indication is confirmed, on a broader statistical basis, by the data shown in Fig. 4b.

(ii) $D \sim \gamma / k_\perp^2$ and Mixing Length Estimates

The $\gamma / k_\perp^2$ models employ the argument that at saturation the destabilising mechanism (usually taken to be proportional to the linear growth rate) is balanced by turbulent diffusion (i.e. $k_\perp^2 D$). Alternatively they correspond to drift wave transport associated with fluctuations whose magnitude is given by the mixing length estimate $e\tilde{\varphi}/T \sim 1/(k_\perp L_n)$. The value of $k_\perp$ is to some extent a free parameter. The spectrum is expected to peak at $k_\perp \rho_s \sim 0.3$ where the linear growth is a maximum and experimental observation is consistent with this. DOMINGUEZ and WALTZ (1987) used this argument to derive the electron and ion thermal conductivities that would be caused by circulating electron drift modes (both collisional and collisionless) and the trapped electron modes. Their simplified treatment of the electron modes has a switch from the collisional to collisionless mode as a collisionality threshold is crossed. (In reality an intermediate collisionality might involve both modes, see HORTON (1976)). The expressions they give are, for the trapped electron mode (collisionless or dissipative):

$$\hat{D}_{te} = \varepsilon^{1/2} \frac{\omega_{*e}}{k_\perp^2} \left\{ 1 \, , \, \frac{\omega_{*e}}{\nu_{eff}} \right\}_{min} \tag{7}$$

The suggested choice of $k_\perp$ is to take $k_\perp \rho_s = 0.3$. This transport coefficient is then combined with the expressions for the circulating modes given earlier (Eqs. (4) and (5)), with adjustable coefficients of order unity, to give a total electron thermal diffusivity. PERKINS (1984) derives identical expressions for the thermal conductivities, by considering a random walk argument for the diffusion in terms of 'step sizes' and the frequency of such a step. The calculations in this section apply to modes for which shear damping is suppressed so they are always unstable.

An alternative $\gamma / k_\perp^2$ estimate of the electron thermal transport due to trapped electron drift modes, given by ROMANELLI et al. (1986), is

$$\chi_e = \frac{5}{2} \varepsilon^{1/2} \frac{\omega_{*e} \omega_{*e}^T}{k_\perp^2 \nu_{eff}} \frac{1}{1 + 0.1/\nu_{*e}} \tag{8}$$

where the function of $\nu_{*e} \equiv \nu_{eff} / \omega_{be}$ has been included to allow a smooth transition from a collisionless to a collisional region. The frequency $\omega_{*e}^T = \eta_e \omega_{*e}$ in this expression yields a factor η_e times the results presented above.

Figure 5 shows that for the trapped electron mode the dissipative regime of Dominguez and Waltz generally applies in JET over most of the plasma cross-section except at the lowest densities. As illustrated in Fig. 6a, an increase of χ^{TH} with radius in the "confinement zone" is prevented by the strong temperature dependence ($\sim T_e^{5/2}$ in the dissipative limit). Additional transport near the plasma boundary would be provided by the addition of the circulating mode contribution (Fig. 3), as proposed by Dominguez and Waltz.

The magnitude of χ^{TH}(TEM) tends to exceed that of χ_{eff}^{EXP}, especially if Eq. (8) is used ($\nu_{*e} \lesssim 0.1$, and $\eta_e > 1$). A comparison with Eq. (7) on a statistical basis is given in Fig. 6b, where local values of the thermal conductivity are plotted as functions of the average input power per particle. All instances with $\chi^{TH} < \chi^{EXP}$ correspond here to high-density plasmas, in which the diamagnetic frequency is strongly reduced by flat density profiles.

TANG (1986) circumvented the discrepancy in the radial variation of χ_e by imposing the experimental radial variation on his transport model. Over a wide range of parameters and heating profiles, the experimental temperature profiles usually tend towards a "consistent" shape, which can be approximated by the form (j = e, i)

$$T_j(r) = T_{jo} \exp\left[-\alpha_T (r/a)^2\right] \tag{9}$$

where Tang chose $\alpha_T = (2/3)(q_{edge} + 0.5)$. He assumed that in the confinement region, between q = 1 and 2, the transport results from the microinstabilities considered here and in CONNOR et al. (1993), while outside this region some other mechanism, as yet unknown, becomes dominant. Writing $\chi_j(r) = \chi_{jo}F(r)$, the radial variation F(r) required to produce the consistent profile shape can be evaluated from the energy balance equation. Hence only its magnitude χ_{jo} remains to be determined. This is done by equating a weighted mean value of $\chi_j F(r)$ and the predicted $\chi_j(r)$ over the region where $1 < q < 2$. The aim of this transport model is to predict T_{jo}, the magnitude of the consistent temperature profile, for specified density and heating profiles. Its scaling should follow that for whichever instability occurs in the confinement region.

In the case of the trapped electron mode, for which Tang adopts an expression similar to Eq. (8), it is apparent from Fig. 6 that, in addition to the radial "rearrangement" for χ^{TH}, a sizeable reduction in magnitude is required to match the JET data.

(iii) Weak Turbulence Estimates

GANG et al. (1991) present a weak turbulence calculation of the transport expected from the trapped electron driven drift wave. The mode structure is that of the sheared slab and two collisionality regimes are considered: collisionless $\omega > \omega_{de} > \nu_{eff}$ and dissipative $\nu_{eff} > \omega > \omega_{de}$, where $\omega_{de} = (k_\theta \rho_s) c_s / R = \varepsilon_n \ \omega_{*e}$ is the magnetic drift frequency and ω is the mode frequency. The trapped electrons are constrained to satisfy

$$(\nu_{eff}, \omega_{de}, \omega) < \omega_{be} \qquad (10)$$

where ω_{be} is the trapped electron bounce frequency. A kinetic treatment is employed whereby the ions are described by the nonlinear gyrokinetic equation, the trapped electrons by the nonlinear bounce-kinetic equation and the untrapped electrons are assumed to be adiabatic. Ion and electron temperature gradients are neglected. The fluctuation spectrum is derived by balancing the linear growth rate, the shear damping and the non-linear energy transfer due to non-linear ion Landau damping. From this spectrum it is possible to derive the following transport coefficient

$$\chi_e = 0.8\tau^{-3/2}\left(\frac{L_n}{L_s}\right)^{1/2}\left(A_e^l \frac{\bar{\gamma}}{\hat{s}}\right)^2 H\left(\bar{k}_\theta^c\right)\frac{\rho_s^2 c_s}{L_n} \qquad (11)$$

where

$$A_e^l = \sqrt{\varepsilon}(L_n / L_s)^{1/2} \ell n \left(\hat{s}\sqrt{\frac{L_s}{L_n}} \ k_\theta \rho_s\right),$$

the variable $\bar{\gamma}$ is a measure of the linear electron drive given by

$$\bar{\gamma} = \begin{cases} \varepsilon_n^{-3/2} e^{-1/\varepsilon_n} & \text{collisionless} \\ c_s / (\nu_{eff} \ L_n) & \text{dissipative} \end{cases}$$

and H $(\bar{k}_\theta^c)$ is a function of the cut-off in the wave number spectrum due to shear damping, obtained by solving the equation which matches the linear electron drive of the mode to the shear damping (i.e. the nonlinear transfer rate is neglected). Stable JET discharges would thus be excluded.

As discussed above, only the dissipative limit is in practice relevant for JET plasmas (where normally $\varepsilon_n < 1$). We have also shown that the constraint Eq. (10) is easily satisfied. The model Eq. (11) is applicable where the argument of the logarithm in A_e^ℓ is greater than unity i.e. $\hat{s}^2 \; L_s / L_n > 1$; this generally excludes the low-shear plasma core. In the case shown in Fig. 7a, this condition is only satisfied for $\rho \geq 0.4$. In this region, the complicated functional dependences in the model by Gang et al. lead to a non-monotonic χ_e which, as anticipated by the authors, is lower than the predictions of the mixing length theories. The correlation with JET data is not particularly good. As an example, Fig. 7b illustrates the strong decrease in χ_e^{TH} with increasing density, due to the dependences on L_n and ν_{eff} in Eq. (11).

A similar theory is given by ROGISTER (1989) who finds the following form for the electron heat flux q_e

$$\frac{q_e}{p_e} \sim c_s \frac{\rho_s^2}{L_s^2} \frac{L_n}{L_s} \frac{T_i}{T_e} \Gamma^* \left[G\left(\Gamma^* - 1\right)\right] k_\theta \rho_s \qquad (12)$$

where p_e is the electron pressure and G is an unspecified function of $\left(\Gamma^* - 1\right)$, which increases sufficiently fast that the plasma adopts 'marginal stability' profiles corresponding to $\Gamma^* = 1$. For $\hat{s}^2 \; L_s / L_n > 1$, which is the limit relevant to the confinement region of JET plasmas, the instability is present when

$$\Gamma^* = \lambda \frac{\varepsilon^{1/2} \eta_e}{k_\theta \rho_s} \sqrt{\frac{L_s}{L_n}} \frac{1}{\hat{s}} \frac{\omega \nu_{eff}}{\left(\omega^2 + \nu_{eff}^2\right)} > 1 \qquad (13)$$

where λ is an adjustable numerical coefficient and $\omega / \nu_{eff} = 8.86 \cdot 10^{13}\, \varepsilon T_e^2 / \left[A_i^{1/2} n L_n (1 + Z_{eff})\right]$. (An expression for Γ^* in the opposite limit of very low shear is given in ROGISTER et al. (1988)).

The difference between this result and that presented by GANG et al. (1991) is due to the fact that GANG et al. neglect the electron temperature gradient; also, they treat the trapped electrons nonlinearly, but the resulting effects are found to be small.

Figure 8 shows that, for typical plasma conditions in JET, the stability parameter Γ^* has a strong radial variation; the outer part of the plasma column, where global confinement is mostly determined, is generally found to be stable. In fact, given the uncertainties in determining Γ^* itself using experimental data, one might even interpret Figure 8b as indicating that at $\rho = 0.8$ the plasma is being kept at marginal stability. This appears however to be unlikely since, even leaving aside the Γ^*-dependent factors, Eq. (12) gives in this region a very low level of transport ($\chi_e^{TH} \lesssim 0.1\ m^2/s$, and decreasing with radius, for $k_\theta \rho_s \sim 1$).

(iv) Toroidal Mode Structure

When the toroidal magnetic drifts are taken into account there exists an extra, toroidicity induced, branch of the drift wave [CHEN and CHENG (1980)]. Of course, the original slab-like mode still exists, though it will be modified slightly. SIMILON and DIAMOND (1984) suggest that it is the toroidal branch of drift modes which is important and always unstable. They develop the non-linear theory of these modes and apply it in particular to the trapped electron driven drift waves. They consider a linear electron response which is taken to be in two parts: an adiabatic part and a nonadiabatic part which is modelled by an 'iδ' prescription representing trapped electron drive. The ions are described using the nonlinear gyro-kinetic equation. Calculation of the fluctuation levels and spectrum (in a strong turbulence regime) leads to the following forms for the test particle diffusion coefficients. For the untrapped electrons,

$$\chi_e \sim D_u = 0.2 \frac{v_*^2}{\omega_{te}} \frac{(2\varepsilon)^{1/6}}{\hat{s}^{7/3}} \left(\frac{v_* \rho_s^{-1}}{\nu_{eff}} \right)^{1/3} \tag{14}$$

where $v_* = \omega_{*e} / k_\theta = T_e / eBL_n$. For the trapped electrons, two collisionality regimes are considered. In the dissipative regime $\nu_{eff} > 2\varepsilon_n \omega_{*e}$

$$\chi_e \sim D_t = (2\varepsilon)^{1/2} D_u \frac{\omega_{te}}{\nu_{eff}} \tag{15}$$

where an upper bound on the collisionality, $\nu_{eff} < \omega_{be}$, is imposed due to the form chosen for δ. In the collisionless regime $\nu_{eff} < \omega_{de}$

$$\chi_e \sim D_t \sim (2\varepsilon)^{1/2} \frac{v_*^2}{\pi^2 \hat{s}^2 \omega_{de}}. \tag{16}$$

A comparison with JET data (Fig. 9) shows that all three diffusion coefficients exhibit an incorrect radial behaviour (the unfavourable shear scaling adding to the usual temperature dependence), with a correspondingly large excursion in magnitude. The disagreement is similar to that characterizing many ∇T_i-driven turbulence theories of anomalous ion heat transport, discussed in detail in CONNOR et al. (1993).

A weak turbulence calculation of the transport due to the toroidal collisionless trapped electron mode has been performed by HAHM and TANG (1991). The work which we have described above considered only the ions to have a nonlinear response and the electrons were treated linearly. Hahm and Tang treat both the ions and the trapped electrons nonlinearly (the circulating electrons are assumed to have a Boltzmann response), describing the trapped electrons by a bounce-averaged drift-kinetic equation and the ions through the gyro-kinetic equation. They argue that the most relevant collisionality regime is the collisionless case, which leads to the ordering:

$$\nu_{eff} < \omega_{De} < \omega_{*e} \quad , \qquad \omega_{bi} < \omega < \omega_{be} \tag{17}$$

where ω_{De} is an orbit-averaged precession drift frequency. The constraint $\omega > \omega_{bi}$ allows the effects of trapped ions to be neglected. Using weak turbulence theory to calculate the fluctuation spectrum, Hahm and Tang derive an electron thermal conductivity given by:

$$\chi_e \approx \left(\frac{2^7 \varepsilon}{15}\right)\left(\frac{\tau q^2}{\hat{s}^2}\right)\left(1+\frac{5}{4}\eta_i\right)^{-1} F\,(\,\varepsilon_n,\ \hat{s})\frac{\rho_s^2 c_s}{L_{Te}} \tag{18}$$

with

$$F = \left(\frac{R}{L_n}\right)^2\left(\frac{R}{GL_n}\right)^4\left(\frac{R}{GL_n}-\frac{3}{2}\right)^2 \exp\left(-\frac{2R}{GL_n}\right),$$

where (TANG (1990)) $G(\hat{s}) = 0.64\ \hat{s} + 0.57$.

For the small set of low density JET plasmas to which the model is applicable (see Eq. (17) and Figure 5b), the predicted χ_e is found to be more than one order of magnitude larger than the observed χ_{eff}^{EXP}.

(v) Transport Stabilisation

KAW (1982) considers the effects that the anomalous thermal transport itself has on the stability of the collisionless trapped electron mode. He finds that for values of χ_e which are sufficiently high, the transport has a stabilising influence on the mode, i.e. the instability becomes self-stabilising. Kaw illustrates the idea with a relatively simple model of the trapped electron mode. He considers $\nu_{*e} < 1$ and a fluid description of the ions, with the passing electrons taken to be Boltzmann-like. The response for the trapped electrons is calculated from a model equation which includes the effect of transport on the trapped electron distribution function. This leads to a growth rate for the resulting mode of the form:

$$\gamma \sim \frac{\omega_{*e}^2}{k_\perp^2 \chi_e}$$

It can be seen that χ_e plays a similar role to that played by the effective collision frequency in the dissipative trapped electron mode. The level at which χ_e saturates is then assumed to be given by marginal stability, i.e. this growth of the mode is balanced by the shear damping, leading to the following expression for the electron thermal diffusivity:

$$\chi_e = \frac{\alpha\varepsilon^{1/2}}{k_\perp^2} \frac{\omega_{*e}}{\left(1+k_\perp^2\rho_s^2\right)^2} \frac{L_s}{L_{Te}} \tag{19}$$

where Kaw suggests that $k_\perp \rho_s \sim 1$. The parameter α is an 0(1) number describing an averaging over the velocity distribution.

In Fig. 10, Eq. (19) has been used with $\alpha = k_\perp \rho_s = 1$. The predicted transport has the right order of magnitude, and for high-density plasmas remains at all radii within a factor ~ 3 of the observations. At low density there is a more serious overestimate in the hot core region. As for previously discussed results, with a leading term $\chi_o^{TH} \sim c_s\rho_s^2 / L$ (with $L = L_n$, L_T or L_s) an additional effective 1/L-dependence would be required here in order to produce the desirable radial increase of transport.

2.4 Inverted Gradient Profile Effects

Inverted gradient profiles (i.e. negative η_e, η_i) have different effects on plasma stability depending on whether the mode under consideration is the circulating electron mode or the trapped electron mode. The circulating mode is destabilised relative to the positive $\eta_{i,e}$ case, whereas the trapped mode is stabilised (TANG et al. (1975)). Thus there is a competition between the two types of mode and we might expect the overall result to be stabilising when the collisionality is low (and trapped electron effects are important) and destabilising for higher collisionality (when they are negligible).

HORTON (1976) investigates this effect by constructing a dispersion relation which describes all three modes (i.e. collisional and collisionless circulating modes and the trapped mode). He finds that for $\eta_{i,e} < 0$ there is a gain in stability (over the positive $\eta_{i,e}$ case) when $\nu_{*e} < 0.3$ and a destabilisation when $\nu_{*e} > 1$. These linear results are then used to derive a quasi linear estimate of the transport that might be expected from a plasma in which all three instabilities exist. The resulting expressions for the particle and heat fluxes are rather complicated. Considering the dissipative mode BISHOP and

CONNOR (1990) simplify Horton's expression to derive the electron thermal conductivity

$$\chi_e = \frac{1}{8\sqrt{\pi}} \frac{q}{\varepsilon_n v_{*e}} \left(\frac{L_s}{L_n}\right) \left(\frac{m_e}{m_i}\right)^{1/2} \frac{\rho_s^2 c_s}{L_n} \left(15 + \eta_e^{-1}\right) \tag{20}$$

The data base of JET plasmas with negative η_e is essentially limited to medium- or high-density H-mode discharges. For the example shown in Fig. 11a, $\nabla n_e > 0$ from the magnetic axis up to $\rho \sim 0.8$, while v_{*e} approaches or exceeds unity and $\eta_e \leq -1$ throughout that region. Fig. 11b shows that Eq. (20) does not adequately describe the transport observed in this regime.

2.5 Short Wavelength Trapped Electron Mode

An analysis of the short wavelength trapped electron temperature gradient driven mode is given by DIAMOND et al. (1990). This short wavelength limit allows the ions to be treated as Boltzmann (imposing the restriction $k_\theta \rho_s > 1$). An upper bound on k_θ is obtained by requiring that trapped electron effects are important, i.e. $\omega_r < \omega_{be}$, where ω_r is the real part of the mode frequency. The mode frequency is of the order ω_{*e} so that we are concerned with the wavelength range:

$$1 < k_\theta \rho_s < \frac{\varepsilon^{1/2} \varepsilon_n}{q} \left(\frac{m_i}{m_e}\right)^{1/2} \tag{21a}$$

Collisions are neglected, which leads to the constraint:

$$\frac{k_\theta \rho_s c_s}{R} > v_{eff} \tag{21b}$$

A linear dispersion relation is derived where the passing electrons are treated as Boltzmann-like and the trapped electrons are described by a bounce-average of the drift-kinetic equation. From this dispersion relation, a criterion for instability, the mode frequency, $\omega_r = F(\varepsilon, \tau)\omega_d$ and the growth rate, $\gamma = G(\varepsilon, \tau, \varepsilon_T)\omega_d$ are derived. These are then used in the 'mixing length' expression for the electron thermal conductivity:

$$\chi_e = \frac{G}{F} \frac{\omega_d}{(k_\theta \hat{s})^2} \tag{22}$$

As we have discussed earlier, the collisionless limit Eq. (21b) generally does not apply in JET. However, a linear analysis of the short wavelength limit of the dissipative trapped electron instability was performed by MIKHAILOVSKII (1976). The limit considered is such that the wavelength of perturbations is small in comparison with the ion Larmor radius, i.e. $k_\perp \rho_s >> 1$. Again, there presumably exists an upper bound (i.e. Eq. (21a)) which is derived from assuming that the trapped electron effects are important. The growth-rate which he derives leads to the instability criterion $\eta_e > 1.52$, which is generally satisfied in JET across most of the plasma cross-section.

No expression for the transport is given in this work, but using the mixing length expression of Eq. (22), with the values of growth rate and mode frequency derived by Mikhailovskii, we obtain the result shown in Fig. 12. Upper and lower limits on χ_e^{TH} correspond here to the extremes of Eq. (21a).

3. ELECTRO-MAGNETIC FLUCTUATIONS

Transport theories which involve electro-magnetic fluctuations on the collisionless skin-depth scale c/ω_{pe} are attractive because they can reproduce the linear scaling of the confinement time with density observed in the Alcator tokamak (OHKAWA (1978)). This Section summarises the models which fall into this class of (c/ω_{pe})-type turbulence. In the next subsection we describe theories in which no specific source for the electro-magnetic fluctuations is given. Instead the fluctuations are merely assumed to exist and to be sufficiently large that the plasma is strongly turbulent; it is shown that such a system exhibits transport due to stochastic motion that is insensitive to details of the source of the fluctuations. We then discuss the possibility that it could be an electron temperature gradient driven mode that is responsible for these magnetic fluctuations.

3.1 General Electro-magnetic Fluctuations

Provided the fluctuations are sufficiently large it is possible to get stochastic transport of particles. HORTON (1985), PARAIL and YUSHMANOV (1985) and HORTON et al. (1987) derive the requirements for stochastic motion and the implications such a motion has for transport levels. Without specifying the source of the electro-magnetic fluctuations (but postulating that they could originate from electron drift waves) they assume that a state of strong non-linearity exists and that the system is describable in terms of a chaotic distribution of vortical flows. The equations of motion of particles under the influence of a model spectrum of electro-magnetic fluctuations are solved numerically and a diffusion coefficient *D* is calculated. It is found that *D* is relatively insensitive to properties of the fluctuation spectrum.

In a random walk estimate of the diffusion coefficient arising from the electro-static part of the fluctuation spectrum of a highly turbulent plasma of the type discussed above, the relevant frequency is the circulation (or **E** x **B** trapping) frequency Ω_E and the step-length is $k_\perp^{-1}$. The dominant contribution to the transport is through the trapped electrons, because they do not experience the whole variation of the perturbation along **B**, so that

$$\chi_e \sim \varepsilon^{1/2} \frac{\Omega_E}{k_\perp^2}$$

In his analysis, HORTON (1985) showed that a condition for stochasticity is $\Omega_E \sim \Delta\omega$ where $\Delta\omega$ is the spread in frequency of the driving instability at a given wave number. For electron drift waves

$$\Delta\omega \sim \omega_{*e} = k_\perp \rho_s \frac{c_s}{L_n}$$

and the corresponding wavelength is $k_\perp \rho_s \sim 1$, so that

$$\chi_e^{(1)} \sim \varepsilon^{1/2} \rho_s^2 \frac{c_s}{L_n} \qquad (23)$$

Although there may be some modification to this through the details of the fluctuation spectrum, the numerical study which was described above suggests that their effect will be small.

The regime considered by PARAIL and YUSHMANOV (1985) corresponds to shorter wavelength (electro-magnetic) modes, with $k_\perp \sim \omega_{pe}/c$. They consider that stochasticity occurs when $\Omega_E \sim \omega_{be}$, where ω_{be} is the bounce frequency of trapped electrons, which leads to a test particle diffusion rate of

$$\chi_e^{(2)} \sim \varepsilon^{1/2}\left(\frac{c}{\omega_{pe}}\right)^2 \omega_{be}. \tag{24}$$

Assuming that both parts of the fluctuation spectrum will be present with sufficient amplitude to produce stochastic diffusion allows a total diffusion rate to be written as

$$\chi_e = \varepsilon^{1/2}\left\{\rho_s^2 \frac{c_s}{L_n} \hat{D}_1(\alpha) + \left(\frac{c}{\omega_{pe}}\right)^2 \omega_{be}\hat{D}_2(\alpha)\right\} \tag{25}$$

where $\hat{D}_{1,\,2}(\alpha)$ represent slowly varying functions of the parameter set $\{\alpha\}$ which defines the fluctuation spectrum. $\hat{D}_{1,\,2}(\alpha)$ can be treated as adjustable constants of order unity when comparing this formula with experiment. However, there does exist a significant variation with the magnetic shear and KESNER (1989) has obtained the following fit:

$$\hat{D}_{1,2}(\alpha) \propto \left(0.05 + 0.65e^{-3|s_\ell|}\right) \tag{26}$$

where s_ℓ is the local shear on the outside of the torus.

Figure 13a indicates a good level of agreement between the theoretical coefficients of Eqs. (23) and (24) and the observed χ_{eff}, over much of the plasma cross-section, both in magnitude and in radial dependence. A linear combination such as Eq. (25) could thus provide an acceptable description of the data in this case. (Note, however, that inclusion of the shear dependence of Eq. (26) would make the agreement worse near the plasma edge). An in-depth assessment of $\chi_e^{(1)}$ and $\chi_e^{(2)}$ will be given below, but first we discuss briefly the possible additional effect of collisions on the predicted transport.

The work described so far considered a collisionless plasma and assumed that the trapped electron diffusion is dominant over the passing electrons. If the collisions of electrons with ions are included, then trapped electrons are converted to passing ones at a rate which is proportional to the effective collision frequency of the electrons. KIM et al. (1990) generalise the results of HORTON et al. to the following form:

$$\chi_e = \varepsilon^{1/2}\left\{\rho_s^2 \frac{c_s}{L_n}\hat{D}_1(\alpha) + \left(\frac{c}{\omega_{pe}}\right)^2 \omega_{be}\hat{D}_2(\alpha)\right\} + \nu_{ei}\left(\frac{c}{\omega_{pe}}\right)^2 \hat{D}_3(\alpha) \qquad (27)$$

The third term is expected to be important at the edge of tokamak plasmas, where the collisionality can be high. In fact, Figure 13b shows that JET plasmas are too collisionless for this term to contribute significantly to transport, even near the plasma edge. Some other mechanism (for example a strong local ion energy transport) must therefore be invoked to account for the increase in χ_{eff}^{EXP} towards the outer boundary.

New effects can arise when the influence of collisions on trapped electrons in the presence of time varying fluctuations is considered. Using a random walk argument, CONNOR and HASTIE (1993) consider the response of trapped electrons to a wave with $\omega \sim \omega_* > \hat{\nu}$ [with $\hat{\nu} = \nu / \delta$ where δ is the width of the appropriate collisional boundary between trapped and passing electrons]. The decorrelation frequency is given by $\hat{\nu}$, leading to

$$\chi_e \sim \delta^{1/2} \; \hat{\nu}_e \left(\frac{e\phi}{T_e}\right)^2 L_n^2$$

which is maximised by choosing the minimum value of δ consistent with the assumption $\hat{\nu} = \nu / \delta < \omega$. Combining this with a mixing length estimate $e\phi / T_e \sim 1 / k_\perp L_n$ and assuming $k_\perp$ is set by the ion Landau damping condition $\omega \simeq v_{ti} / Rq$.

$$\chi_e \sim \left(\frac{\nu_e c_s}{L_n}\right)^{1/2} \tau\rho_s^2 \left(\frac{Rq}{L_n}\right)^2 . \qquad (28a)$$

This upper limit on χ_e now largely exceeds the observed transport in the confinement region, as can be seen from Figure 13b. An alternative assumption is that the fluctuations have slab-like drift wave structures (PEARLSTEIN and BERK (1969)), which would suggest $k_\perp \sim k_T \sim (L_n / L_s)\rho_s^{-1}$ and hence

$$\chi_e \sim \left(\frac{\nu_e c_s}{L_n}\right)^{1/2} \tau\rho_s^2 \frac{L_s}{L_n} . \qquad (28b)$$

This heat diffusivity, while preserving the main parametric scalings of Eq. (28a), would have a magnitude closer to the experimental χ_{eff} (Fig. 13b).

We now investigate in more detail the properties of the first two terms in Eq. (27). For Figs. 14 and 15 we have selected JET deuterium L-mode data for one particular value of the plasma current (I_p = 3 MA). Figure 14 shows the density dependence of local transport at constant input power. The decrease in χ_{eff}^{EXP} with increasing <n> reflects a favourable scaling of the global thermal τ_E with plasma density; in regression analyses of the total energy replacement time measured by magnetic diagnostics, this trend is usually masked by the presence of energetic particles (more important at low density). The overall behaviour is well described both by $\chi_e^{(2)}$ (whose decrease is mostly due to $\omega_{pe} \propto n_e^{1/2}$) and by $\chi_e^{(1)}$ ($\propto T_e^{3/2} / L_n$, where T_e decreases and L_n tends to increase with increasing density). The discrepancy discussed above concerning the radial variation of χ remains throughout this set of data, as can be seen by comparing the magnitude of χ at ρ = 0.5 and ρ = 0.8 in Fig. 14.

In Fig. 15, data at constant plasma density are examined to identify the dependence of transport on input power (i.e. plasma temperature). The increase in χ_{eff}^{EXP} reflects the global degradation of confinement with increasing additional heating power. This is mimicked by $\chi_e^{(1)}$, because of its strong temperature dependence, while the increase in $\chi_e^{(2)}\left(\propto T^{1/2}\right)$ is clearly less marked.

The comparisons of Figs. 14 and 15 thus confirm that a linear combination such as Eq. (25), with appropriately adjusted constant coefficients of order unity, can lead to a good description of important features of local heat transport in the L-mode regime at JET. (It should be noted that linear scales have been used in Figs. 14 and 15, as opposed to the logarithmic scales of earlier graphs).

It has to be said that there are also aspects of the observed local confinement that clearly cannot be described in a general way by the model Eq. (25). A notable example of these is the transition from Ohmic to additional heating, which in limiter discharges invariably leads to an increase in local heat transport. This transition is often accompanied by an increase in plasma density. In the illustrative example chosen for Fig. 16, this increase is such that the plasma temperature actually remains the same in both regimes. As should be expected, in such a case the increase in χ_{eff}^{EXP} is in stark contrast with the large decrease in $\chi_e^{(2)}$ (and also $\chi_e^{(1)}$ would decrease somewhat due to the flattening of the density profile). This problem was already recognised by PARAIL and YUSHMANOV (1985) who suggested the existence of an additional "heat pinch" term in the energy balance to explain the confinement degradation.

Another shortcoming of model Eq. (25) is its inability to describe the well-established phenomenological improvement of confinement with increasing plasma current. In fact, the q^{-1} dependence of $\chi_e^{(2)}$ would tend to lead to the opposite effect.

To return now to the review of theoretical treatments, PARAIL and POGUTSE (1980) derive an upper bound to the electron thermal diffusivity due to electro-magnetic turbulence, which is assumed to exist on the length scale of the collisionless skin depth c/ω_{pe}. Two expressions for the thermal conductivity are given for odd and even modes respectively (where 'odd' and 'even' refer to the parity of the electro-static potential about a resonant surface). For the odd modes,

$$\chi_e^{(o)} \sim \left(\frac{c}{\omega_{pe}}\right)^2 \frac{v_{te}\hat{s}}{qR} \tag{29}$$

For even modes toroidal coupling to sidebands needs to be taken into account, leading to

$$\chi_e^{(e)} \sim \left(\frac{r}{R}\right)^2 \left(\frac{c}{\omega_{pe}}\right)^2 \frac{v_{te}}{qR} \tag{30}$$

Parail and Pogutse claim that the even modes will, as a rule, be excited before the odd modes and thus $\chi_e^{(e)}$ will be the relevant expression.

Noting that $\chi_e^{(e)} \sim \varepsilon\ \chi_e^{(2)}$, it is clear from the discussion above that Eq. (30) will have a radial dependence now similar to that of the observed χ_{eff}, but will need a numerical coefficient O(10) to match the experimental magnitude. Conversely, since the local shear $\hat{s}$ increases with radius and is of order unity in the confinement region, one would expect $\chi_e^{(o)}$ to provide an even better model than $\chi_e^{(2)}$. Indeed, with a numerical coefficient 0.5 in Eq. (29), Figures 14d and 15d show good agreement with the experimental data.

Finally we consider the work of ZHANG and MAHAJAN (1988), who consider the modes that satisfy $\omega > k_{\parallel} v_{te}$ to be important. The precise form of the mode which might be responsible for driving the turbulence is not addressed, but it is assumed to be such that ω scales like $\tilde{\omega}_{*e}$, where

$$\tilde{\omega}_{*e} = \xi \left(\frac{\omega_{pe}}{c} \right) \rho_s c_s \left(\frac{1}{L_{Te}} + \frac{\alpha}{L_n} \right)$$

i.e. a linear combination of the diamagnetic drift frequency due to both the temperature and density gradients with the perpendicular wavelength being $\sim c/\omega_{pe}$. Little is said about the constants α and ξ, which must be assumed to be parameters of the model to be fixed by comparison with experiment. The length scale is taken to be the collisionless skin depth, thus leading to the following form for the heat diffusivity:

$$\chi_e = \xi \left(\frac{c}{\omega_{pe}} \right) \rho_s c_s \left(\frac{1}{L_{Te}} + \frac{\alpha}{L_n} \right) \tag{31}$$

This expression has parametric dependences that lie between those of $\chi_e^{(1)}$ and $\chi_e^{(2)}$ examined above. A comparison with JET L-mode data yields results similar to Figs. 14b, c and 15b, c, albeit with a less satisfactory radial dependence in χ_e^{TH}. We find that $\xi \simeq 1$ is acceptable for $\alpha = 0$, but $\xi \simeq 0.2 - 0.3$ would be required if $\alpha = 1$ (i.e. if an additional factor $(1 + \eta_e^{-1})$ is included in χ_e^{TH}).

3.2 Electron Temperature Gradient Turbulence

The above work considers the transport due to electro-magnetic fluctuations without specification of their source. GUZDAR et al. (1986) suggest that high frequency drift waves driven by electron temperature gradients could be responsible for the magnetic fluctuations (and therefore anomalous transport) that are observed in tokamaks. The theory of the mode in a sheared slab geometry and its implications for the electron transport are described in the work of LEE et al. (1987). Perhaps a more relevant work as far as tokamaks are concerned is HORTON et al. (1988), in which the nonlinear properties of this electron temperature gradient driven mode are studied in a toroidal geometry. In this section we shall discuss these two theories in more detail.

Let us start with the slab treatment of LEE et al. (1987) which is a more complete description of their original work. Kinetic theory is used in a sheared slab geometry to describe the collisionless electro-magnetic electron temperature gradient driven mode. The equation is solved numerically to analyse the stability. The principal result is that the most unstable mode has a critical $\eta_e \simeq 1$ for instability which is consistent with the shorter wavelength result of HORTON et al. (1988) below. Using quasi-linear theory, they derive the following expression for the electron thermal diffusivity:

$$\chi_e \sim 0.13 \left(\frac{c}{\omega_{pe}}\right)^2 \frac{v_{te}\hat{s}}{qR} \eta_e(1 + \eta_e) \qquad (32)$$

The factor η_e $(1 + \eta_e)$ originates from a numerical fitting of the variation of the maximum value of the mode frequency as a function of η_e, but is restricted to the region $\eta_e(1 + \eta_e) \ll \frac{69}{\tau}$. When comparing with JET data, for which this latter constraint is generally satisfied, we find that Eq. (32) does not fare as well as Eq. (29). The additional η_e-dependent factor introduces much unwanted scatter in the theoretical prediction, and makes the radial dependence of χ_e^{TH} worse again, since η_e tends to decrease at the plasma edge. Also, the transport coefficient Eq. (32) is on average larger than the experimental χ_{eff} by a factor of 2.

The theory of HORTON et al. (1988) mainly makes use of hydrodynamic equations and a tokamak with a circular cross-section is considered. Hydrodynamic theory predicts that there exists a critical value for $\eta_e \simeq 2/3$ above which there is an instability; inclusion of FLR effects raises this value to $\eta_{e,c} \simeq 1$.

The linear theory indicates that the most important η_e driven modes are those with short wavelength and are electrostatic in nature. Under the restrictions for validity of the hydrodynamic treatment, $\omega >> k_{\|}v_{te}$ i.e. $\hat{s}/q < 1/(2\varepsilon_{Te})^{1/2}$, the toroidal regime ($\hat{s} < 2q$) and that the density profile be sufficiently peaked ( ), Horton et al. derive the following mixing length estimate for this short wavelength mode:

$$\chi_e = \left(\frac{m_e}{m_i}\right)^{1/2}\left(\frac{2q}{\hat{s}}\right) \eta_e^{1/2} \frac{\rho_s^2 c_s}{\tau L_n} \qquad (33)$$

In the limit of flat density gradient (i.e. $\eta_e \gg 1$) they give

$$\chi_e = \left(\frac{m_e}{m_i}\right)^{1/2} \left(\frac{2q}{\hat{s}}\right) (2\varepsilon_{Te})^{1/2} \frac{\rho_s^2 c_s}{\tau L_{T_e}}. \qquad (34)$$

As shown in Fig. 17, the level of transport predicted in the confinement region is too low. Due to their temperature scaling, not sufficiently mitigated by the other parametric dependences, the heat diffusivities of Eqs. (33, 34) display the wrong radial behaviour, similarly to many of the drift wave models discussed in Section 2.

However, the longer wavelength part of the spectrum possesses an electromagnetic component, which can give rise to substantial transport when the motion becomes stochastic in nature (HORTON et al. (1987)). Linear theory indicates that in the case of the η_e driven mode there is marginal stability in this long wavelength limit. However, in the non-linear theory a long wavelength mode can be driven unstable through an interaction with two shorter wavelength modes, and the resulting stochastic diffusion leads to two scalings for the transport coefficient, corresponding to the two regimes where stochastic diffusion occurs. For the regime where the circulation frequency of the vortices Ω_E is comparable to the mode frequency,

$$\chi_e \sim \left(\frac{c}{\omega_{pe}}\right)\frac{c_s\rho_s}{L_{Te}}$$

where the typical scale length for the turbulence has been taken to be the skin depth c/ω_{pe} rather than ρ_s as was used in deriving Eq. (23). The behaviour of this transport coefficient has been discussed in Section 3.1 (see Eq. (31)). In the other regime, where the circulation frequency is comparable to the bounce frequency of the trapped electrons, the thermal conductivity $\chi_e^{(2)}$ of Eq. (24) is recovered.

4. RESISTIVE FLUID TURBULENCE

In this section we consider the instabilities of a plasma described as a resistive fluid and indicate the level of transport expected from such instabilities. We shall see that transport can occur from two sources: turbulent convection and a 'stochastic' radial diffusion. The latter is a consequence of the magnetic fluctuations which are predicted to arise because of the instability. These can interact to make the magnetic field stochastic, and induce a subsequent radial transport by parallel motion. In the following subsections we shall consider two types of resistive fluid instability: pressure gradient driven modes and resistivity gradient driven modes.

4.1 Resistive Pressure Gradient Driven Transport

In this subsection we consider the transport which would result because of instability to a resistive ballooning pressure-gradient driven modes of the type considered by CARRERAS et al (1983), not those discussed by DRAKE and ANTONSEN (1985).

The equations describing a plasma as a resistive fluid are invariant under certain sets of scaling transformations of various plasma parameters. This invariance can be sufficient to determine the dependence of the diffusivity on these parameters (CONNOR and TAYLOR (1984)). Consider first the convective loss from fluctuations with toroidal mode number n in the following limit:

$$S >> 1 \quad , \quad n^2/S \ll 1 \quad , \quad \beta q^2/\varepsilon < 1$$

where $S = \tau_R/\tau_A$ with the resistive diffusion time τ_R and the poloidal Alfvén time τ_A defined by $\tau_R = \mu_o r^2/\eta$ and $\tau_A = (\mu_o \rho_m)^{1/2} R_o q/B_o$, $\beta = 2\mu_o p/B^2$, η is the plasma resistivity and ρ_m is the mass density. Assuming that the diffusion coefficient scales as the square of a radial step size to a time step, the invariance transformations lead to the following result for the convective diffusion coefficient:

$$D_c = g_o \frac{\eta}{\mu_o} \left(\frac{\alpha}{\hat{s}}\right) \tag{35}$$

where g_o is a constant and

$$\alpha = -\frac{2\mu_o R q^2}{B^2} \frac{dp}{dr}. \tag{36}$$

As can be inferred from the typical profiles shown in Fig. 18, Eq. (35) gives a very small diffusion coefficient, barely reaching ~ 0.1 m^2/s at the very edge of the plasma.

We now consider the radial transport due to parallel diffusion along the stochastic magnetic field lines (RECHESTER and ROSENBLUTH (1978)). It can be shown that invariance arguments determine

$$D_1 = g_1 \frac{v_{te}^2}{\nu_e} \frac{\varepsilon^2}{q^2 S} \left(\frac{\alpha}{\hat{s}}\right)^{5/2} \tag{37}$$

in the collisional limit $\lambda_{mfp} < L_c$, where L_c is the parallel correlation length of the turbulence. In the collisionless case, $L_c > \lambda_{mfp}$,

$$D_2 = g_2 \frac{R\varepsilon^2 v_{te}}{qS} \left(\frac{\alpha}{\hat{s}}\right)^{3/2} \tag{38}$$

We note that earlier mixing length expressions (CARRERAS et al. (1983)) are largely in agreement with these diffusion coefficients. With numerical coefficients of order unity, both D_1 and D_2 are $\lesssim$ 0.1 m^2/s in the confinement region of typical JET plasma, and so cannot account for any significant part of the observed transport.

Work by CARRERAS et al. (1987) considers the non-linear calculation of the diffusion resulting from the resistive interchange mode. Although such a mode is stable in tokamaks, it is closely related to the resistive ballooning mode and therefore might be expected to show similar characteristics. Comparison with the results of CONNOR and TAYLOR (1984) for this resistive interchange mode enables us to predict how one might expect the ballooning mode driven diffusion (as described above) to be altered if a similar analysis were applied to the equations which describe this mode.

The equations are similar to those considered by Connor and Taylor, apart from two extra terms appearing in the pressure and vorticity evolution equations which are included in order to model an anomalous viscosity μ and cross-field diffusion $\chi_\perp$. The equations are then renormalised and the magnitude of the resulting turbulent viscosity and diffusivity are chosen to make the non-linear dispersion relation marginally stable. The effect is to enhance the diffusivity Eq. (35) by a logarithmic factor:

$$D = \frac{2}{3\pi} g_0 \frac{\eta}{\mu_o} \frac{\alpha}{\hat{s}} \; \ell n \left(\frac{64 r^4}{m^4 q^2 \tau_A^2} \left[\left(\frac{< m^2 >}{m^2} \right)^{1/2} \frac{\mu_0^2 \hat{s}^2}{g_0^2 \eta^2 \alpha} \right] \right) \tag{39}$$

This expression is weakly dependent on the poloidal mode number m ($<m^2>^{1/2}$ is its rms value) and a value for this must be chosen. Numerical simulation by CARRERAS et al. (1987) indicates that the most important m value (i.e. the most unstable m = m_o) is such that $m_o = <m^2>^{1/2}$ and that $<m^2>^{1/2}$ varies with the parameter $\beta/(2\varepsilon^2)$:

$\beta/(2\varepsilon^2)$	$<m^2>^{1/2}$
0.0025	12
0.0050	6
0.0075	3
0.0100	3
0.0125	3

The saturation at $<m^2>^{1/2} \sim 3$ may represent a cascade to long wavelengths ($n \sim 1$) with $<m^2>^{1/2}$ determined by the geometry (i.e. n = 1, q = 3 and m = nq) in which case $<m^2>^{1/2}$ could be assumed to vary like q.

By choosing $m_o = 3$, we find that the logarithmic factor in Eq. (39) is typically O(10). As shown in Fig. 19, this leaves us with a transport coefficient which has the correct radial variation, but negligible magnitude as compared to the measured thermal conductivity.

The heat transport due to stochastic magnetic fields produced by instability to resistive pressure-gradient-driven turbulence is analysed by CARRERAS and DIAMOND (1989) in the collisionless case, who derive an electron thermal diffusivity given by:

$$\chi_e = \frac{1}{2^{13/6}} \frac{1}{<n^2>^{1/3}} \frac{1}{S^{2/3}} \frac{q^2}{\hat{s}} \left(\beta \frac{R_o}{L_p}\right)^{4/3} \frac{v_{te} r^2}{R_o} \tag{40}$$

Here $<n^2>^{1/2}$ represents an rms average of the toroidal mode number for the instability; if it is close to unity, then Eq. (40) yields a transport coefficient that is approximately radially uniform, and within an average factor ~3 of the observed χ_{eff}^{EXP}. The temperature scaling of χ_e^{TH} is compatible with JET L-mode data (compare Figure. 20b with 15a), but the β-dependence in Eq. (40) brings about an unfavourable density scaling (Figure 20c) which is at odds with the clear trend in Figure 14a.

So far we have described the pressure-gradient-driven turbulence through the resistive MHD equations, which are strictly valid only in the short mean free path (Pfirsch-Schlüter) regime. At lower collisionalities (in banana or plateau regimes) trapped particle effects can become important and instability is possible, even in the absence of curvature, due to the bootstrap current and neoclassical viscous damping (CONNOR and CHEN (1985); CALLEN and SHAING (1985)). Because of its role in the driving mechanism, this mode is sometimes referred to as the 'bootstrap current mode'. The non-linear theory and resulting transport has been investigated by KWON et al. (1990) using the same set of neoclassical fluid MHD equations as Callen and Shaing and the techniques of CARRERAS et al. (1987). This leads to the pressure diffusivity:

$$D_p = \frac{1}{8\pi} \frac{\varepsilon}{q} \beta_p \frac{\eta}{\mu_0} \frac{L_s}{L_p} F\left(\varepsilon, \nu_e, \nu_{*e}\right) \tag{41}$$

where F is an algebraic function of aspect ratio and collisionality. This 'neoclassical' instability also gives rise to stochasticity of the magnetic field, and to enhanced electron heat transport:

$$\chi_e \simeq \frac{\chi_e[\text{Eq. (40)}]}{\varepsilon^2 q^{1/3}} G\left(\varepsilon, \nu_e, \nu_{*e}\right) \tag{42}$$

where G is a complicated function which turns out to be approximately constant in radius and of order unity.

Fig. 20a shows that Kwon et al.'s Eq. (41) yields very low transport, while the thermal diffusivity Eq. (42) is significantly larger than the measured one (even when $m_o \gtrsim 3$ is taken into account).

The expressions (35)-(42) are controlled by collisional resistivity, even if neo-classical effects are invoked. A high temperature plasma may be better described by an Ohm's law in which electron inertial effects replace collisional friction. ITOH et al. (1993) have obtained a form for the 'fluid' thermal diffusivity:

$$\chi_e = \frac{v_A}{qR}\left(\frac{c}{\omega_{pe}}\right)^2 \frac{\alpha^{3/2}}{h(\hat{s})}.$$

which can be considered as an analogue of the work of DIAMOND and CARRERAS (1987) for a collisionless fluid rather than a resistive fluid (CONNOR (1993)). Here $v_A = B/\sqrt{\mu_o m_i n}$ is the Alfvén velocity, α is given by Eq. (36) and $h(0) = 1.7$, $h(\hat{s} > 0.7) = 2.5\hat{s}$. A corresponding expression for the effect of electron transport due to the associated stochastic magnetic fluctuations has also been given by Connor, using invariance techniques,

$$\chi_e = \frac{v_{te}}{qR}\left(\frac{c}{\omega_{pe}}\right)^2 \frac{\alpha^2}{\hat{s}}.$$

These forms are valid for 'cold' electrons with $\alpha > m_i\beta_e/m_e$ and are not applicable to JET plasma conditions. (However, it is interesting to note that the Itoh expression does have a promising radial profile, rising at the edge, but would require a multiplicative factor ~ 30.) In the opposite limit $\alpha < m_i\beta_e/m_e$ a kinetic model for the electrons is more appropriate. Nevertheless an effective 'collisionless resistivity' for this situation can still be modelled and forms for χ obtained. Corresponding to the above two equations, Connor has obtained

$$\chi_e = \frac{v_{te}}{qR}\left(\frac{c}{\omega_{pe}}\right)^2 \alpha \qquad (43a)$$

and

$$\chi_e = \frac{v_{te}}{Rq}\left(\frac{c}{\omega_{pe}}\right)\frac{\alpha^{3/2}}{\hat{s}^{1/2}}\rho_s \qquad (43b)$$

for the effects of turbulent electrostatic and magnetic fluctuations respectively.

The thermal conductivity of Eq. (43a) is $\chi_e^{(2)} \cdot (\alpha/\varepsilon)$, where $\alpha = 0(10^{-1})$ increases modestly with radius in the confinement region (Figure 18). As shown in Figure 21, therefore, this χ_e^{TH} is smaller in magnitude, has a less favourable radial dependence, but scales more similarly to the data with the input power, owing to the linear dependence on the pressure gradient in α. In addition, importantly, χ_e^{TH} from Eq. (43a) will lead to an improvement in confinement with increasing plasma current (since $\alpha \sim q^2$), thus reproducing another experimentally observed trend. Conversely, the dependences of Eq. (43b) on shear and temperature (with the gyroradius $\rho_s \sim T^{1/2}$ replacing a collisionless skin depth $c/\omega_{pe} \sim n^{-1/2}$) lead to a radial behaviour at odds with observations, as can be seen in Figure 21a.

4.2 Resistivity Gradient Driven Transport

Resistivity gradient driven turbulence can result from two sources: a gradient in the electron temperature or a gradient in Z_{eff} (i.e. an impurity density gradient). The instability caused by an electron temperature gradient resulting in a radial variation of the resistivity is often called the rippling mode. This mode has a resistive MHD nature and is driven by a radial gradient in the current, which exists as a consequence of the resistivity gradient. A high electron collisionality is necessary in order to overcome the stabilising influence of the parallel electron thermal conduction.

Numerical calculation (HASSAM and DRAKE (1983)) indicates that the rippling mode is unstable for

$$T_e < \frac{3.08 \times 10^4}{\left(k_y L_{Te}\right)^{2/3}}\left[\frac{B^2 L_{Te}}{T_{0e}^{3/2}}\left(\frac{L_s}{q_0 R}\right)\right]^{2/3}$$

with $k_y L_T \sim m$, the poloidal mode number. Here, the units are SI except for temperature which is measured in eV. The subscript zero indicates the parameter measured at the plasma centre. For JET parameters this critical temperature is of the order of 10 eV and therefore the mode will only exist right at the plasma edge (if at all). The transport due to turbulence induced by the rippling mode has been analysed by GARCIA et al. (1985).

As mentioned earlier, a radial variation in the impurity concentration can also give rise to a resistivity gradient and thus affect transport due to the rippling mode. Impurities were included in the analysis of HAHM et al. (1987) and THAYER and DIAMOND (1987) where it was found that their effect is to give an additive contribution to the total transport due to resistivity gradient driven turbulence. The general lack of accurate measurements of the local impurity distribution in JET plasmas prevents us from carrying out quantitative assessments of these theories.

The above analyses of the resistivity-gradient-driven mode employ the reduced resistive MHD equations which are strictly only valid in the Pfirsch-Schlüter collisionality regime. KWON et al. (1989) perform a calculation of the transport due to the mode using neoclassical equations, which are relevant for a description of a plasma in the banana/plateau collisionality regimes. The principal difference between this calculation and those of reduced MHD is that the resistivity in the banana regime becomes dependent on the plasma density as well as the temperature, and thus the rippling mode (which, as described earlier, is driven by a resistivity gradient) is now able to tap the free energy source of the density gradient. Impurity gradient effects and the effects of radiative cooling are not included. Also, it should be noted that diamagnetic ω_{*e} terms are dropped. One-point renormalisation theory is used to derive

$$\chi_e = \left[\left(\frac{3}{2}\eta_e + C_n(1-2\eta_e)\right)\left(\frac{cE_{\parallel}L_s}{BL_n}\right)\right]^{4/3}\left[\chi_{\parallel}k'_{\parallel}{}^2\right]^{-1/3} \qquad (44)$$

where $\chi_{\parallel}$ is the electron parallel thermal conductivity and C_n is a function of the plasma collisionality. This turbulent energy transport is absolutely negligible in plasma conditions of practical interest for JET (where $\chi_{\parallel} \sim 10^{11} \chi_{i,\,neocl}$).

5. TRANSPORT INDUCED BY MAGNETIC ISLANDS

If microscopic magnetic islands of width w_m exist on rational surfaces $m = nq$, they can produce stochastic magnetic fields if islands on adjacent rational surfaces overlap. This then leads to rapid electron thermal transport as the electrons follow the stochastic field lines (RECHESTER and ROSENBLUTH, 1978). It is possible to express the resulting diffusivity in terms of N, the number of toroidal modes whose sum contributes to the stochasticity condition (WHITE and ROMANELLI, 1989).

$$\chi_e = \frac{v_{te}R}{q^3\hat{s}^2}\left(\frac{r}{R}\right)^2\left(\frac{\alpha_s}{N}\right)^3 \tag{45}$$

where $\alpha_s \simeq 1$ is the stochasticity parameter. This expression requires $N \sim 10^2$ to give the correct order of magnitude for χ_e^{TH} at $\rho = 0.5$, and even then features an extremely strong unfavourable radial variation, with unhelpful dependences on both q and the shear.

Equation (45) is generic, independent of the mechanism producing the islands. Tokamaks tend to be linearly stable to the micro-tearing modes that would lead to such islands, but a number of non-linear theories have been developed that provide an explanation for their presence. These theories balance island drive due to currents associated with the presence of the islands against the natural stability from Δ' at high m, to yield expressions of the form

$$w_m = \frac{r w_0}{m}. \tag{46a}$$

Different expressions for the dimensionless quantity w_o are given below.

One can then estimate an electron thermal diffusivity from the Rechester-Rosenbluth formula.

$$\chi_e \sim \frac{v_{te}}{L_s}\frac{m w_m^3}{r} \tag{46b}$$

where $m \gtrsim 10^2$ is a typical mode number. One possible mechanism is the bootstrap current driven island (CARRERA et al., (1986)) for which

$$w_0 \;=\; 1.2\left(1-\varepsilon^{1/2}\right)^2 \varepsilon^{3/2}\frac{\beta_p R}{\hat{s}L_n} \tag{47}$$

where we use a finite aspect ratio value for the neoclassical resistivity (WESSON, 1987). Another source of magnetic island drive arises from the currents associated with finite ion Larmor radius effects (SMOLYAKOV (1989); SAMAIN (1984); REBUT and HUGON (1991)). Smolyakov considers the electrons to be described by Braginskii equations and finds

$$w_0 \;=\; \frac{\beta L_s^2}{L_n^2}\eta_e\left(\eta_e - 1\right) \tag{48}$$

for islands with $m \sim r/\rho_i$. Samain finds for similar m values

$$w_0 \;=\; 0.3\frac{\beta L_s^2}{L_n^2}\eta_e\left(1+\frac{\eta_e}{4}\right). \tag{49}$$

Rebut and Hugon obtain the same scaling as eqn. (49) but have a coefficient 4.

By combining Eqs.(47-49) with Eqs. (46), we find thermal diffusivities having very large values in the plasma core and vanishing towards the edge (Figure 22), mostly as a result of the β-dependence of w_0.

SMOLYAKOV and HIROSE (1993) have also considered the collisionless case when electron inertia replaces resistivity in the Ohm's law. The theory assumes fluid electrons and leads to magnetic islands of width

$$w \sim \left(\frac{c}{\omega_{pe}}\right)\frac{\left(1+\eta_e/2\right)^{1/2}}{\eta_e^{1/2}}$$

The condition that the electrons are fluid $\omega >> k_{\|}' w\, v_{te}$ requires $\beta_e L_s^2 / L_n^2 >> 1$. The resulting expression for transport due to stochastic magnetic fields is

$$\chi_e = \left(\frac{c}{\omega_{pe}}\right)^2 \frac{v_{te}}{qR}\frac{\left(1+\eta_e/2\right)}{\eta_e}\hat{s}. \tag{50}$$

This thermal conductivity is very similar to that of Eq. (29) derived by PARAIL and POGUSTE (1980) in the case of electro-magnetic turbulence. As was discussed in Section 3.1 (see Figures 14d and 15d), it can reproduce some important features of L-mode transport, although not the favourable scaling with current. In addition, the η_e-dependence in Eq. (50) provides a desirable factor that increases towards the edge (where η_e generally falls below 1). Unfortunately, the assumption of fluid electrons is not warranted for JET plasmas, where $\beta_e(L_s / L_n)^2 \sim 10^{-1}$, and the applicability of Eq. (50) remains to be proven.

KADOMTSEV (1991) has considered the transfer of energy from ions to magnetic islands with w << ρ_i, as they pass through them. He finds the ions can pump the islands if these are 'slanted' relative to the magnetic surfaces in a torus. Balancing this pumping against the electron dissipation associated with electron inertia yields a saturated island width. Kadomtsev distinguishes two situations: at low levels of heating

$$\chi_e \sim \varepsilon^{3/2} \frac{v_{te}}{qR} \left(\frac{c}{\omega_{pe}} \right)^2 \tag{51}$$

while for higher heating powers

$$\chi_e \sim C \, \frac{v_{ti}}{R^2} \, r^3 \beta_\theta \tag{52}$$

where C is a small constant.

In Eq. (51), $\chi_e^{TH} = \varepsilon^{1/2} \, \chi_e^{(2)}$, where $\chi_e^{(2)}$ has properties that were assessed in Section 3.1 by comparison with JET L-mode data. Here it is proposed to apply the expression to the case of Ohmic heating only; Figures 23a, b show that Eq. (51) yields the correct magnitude for χ_e, and a density scaling which is compatible with observations. The unfavourable current scaling of χ_e^{TH} is, however, in contrast with the experimental evidence.

Expression (52) also gives the correct magnitude for χ_e, when compared with JET data in the presence of auxiliary heating. An assessment such as that carried out in Figures 14 and 15 for previously discussed models shows that the observed power degradation of confinement is acceptably reproduced, while at constant power χ_e^{TH} is practically independent of the plasma density (which may still be compatible with the data in Figure 14a, bearing in mind the difference between χ_{eff} and χ_e). The linear dependence of χ_e^{TH} on β_θ in Eq. (52) implies a decrease in transport near the plasma edge (in spite of the strong scaling with minor radius), but at the same time yields the desirable improvement in confinement with plasma current, as illustrated in Figure 24.

Transport due to micro-tearing mode has been considered by GARBET et al. (1990). In the collisionless regime these modes are linearly stable but can be non-linearly destabilised by radial diffusion, allowing a self-consistent solution with turbulent diffusion. A typical upper bound to the resulting thermal diffusivity is

$$\chi_e \leq 0.05 \ \rho_i^2 \frac{v_{te}}{L_s}. \qquad (53)$$

This is similar to $\chi_e^{(1)}$ that was discussed in Section 3.1, except for the shear length replacing the density scale length and for the missing factor $\varepsilon^{1/2}$. As a result, Eq. (53) yields a weaker radial dependence, a weaker density scaling than in Figure 14b and, inappropriately, a current scaling opposite to what is commonly observed.

6. DISCUSSION AND CONCLUSIONS

Theoretical expressions for the electron thermal diffusivity χ_e published in the plasma physics literature have been systematically compared with values of a one fluid effective thermal diffusivity χ_{eff} taken from JET data. Before discussing the results, we comment on some points concerning the technique used for comparing theoretical models with experimental data.

(i) The use of a one-fluid "effective" experimental thermal conductivity makes any assessment of a theoretical model for electron heat transport approximate, in the sense that one should not expect χ_e^{TH} to reproduce exactly the same trends and magnitude as χ_{eff}^{EXP}. On the other hand, it seems reasonable to assume that trends in χ_e^{TH} should not systematically contradict those observed for χ_{eff}^{EXP}; nor should the predicted magnitude of

χ_e be largely in excess of that of χ_{eff}^{EXP}. Indeed, theoretical models often predict similar scalings for χ_e and χ_i. (When the predicted electron heat diffusivity is negligible as compared to χ_{eff}^{EXP}, then the theory may be valid, but does not help understanding anomalous transport in JET). These disadvantages are offset to some extent by the fact that the uncertainty in the determination of χ_{eff}^{EXP} is usually much lower than that affecting separate estimates of χ_e^{EXP} and χ_i^{EXP} (which are only rarely possible, anyway, as discussed in CONNOR et al. (1993)). We have found that for many theoretical models $\chi_e^{TH} << \chi_{eff}^{EXP}$ in the outer plasma region. It is of course possible that ion heat transport systematically dominates near the edge. However, the study in **Part I** comparing models for the ion heat transport (CONNOR et al. (1993)) did not find any convincing theoretical model which could reproduce the experimental heat flux.

(ii) The JET experimental data used for most comparisons refer to standard L-mode discharges. These are the most common type of plasma, and the ones for which the widest portion of parameter space is explored. We have assumed that any good model must be able to reproduce basic properties of such L-mode plasmas, before one can consider application to more special confinement regimes.

(iii) All models have been examined (when found to be applicable) in the following fashion: first, by a local comparison with one representative set of plasma conditions, to assess the magnitude and radial trends of χ_e^{TH}; then, if this test leads to plausible results, by comparing variations with respect to one or more of the relevant parameters, such as density or power. Such tests are clearly not exhaustive; even in those cases where acceptable agreement was found, one would still require validation of the theoretical modes by transport code simulations, with comparisons between predicted and measured plasma profiles. This is especially relevant for the (many) models that involve nonlinear relationships between fluxes and driving gradients.

We now draw some general conclusions from the detailed comparisons we have made. Concerning the specific "ingredients" that can make theoretical expressions for χ_e more appealing candidates for the description of the observed transport we note that:

(i) Any model of the pure gyro-reduced Bohm type, with $\chi_e \sim c_s\rho_s^2 / L$, given by a number of the drift wave models, will tend to yield the correct degradation of confinement with power. A radial dependence $\sim T^{3/2}$ is however in disagreement with observations, and we find that even having $L = L_n$, or L_T, both of which decrease with radius, generally is not sufficient.

An additional radially increasing factor is required, and models that have χ_e proportional to q or q^2 fare best because they simultaneously introduce a favourable dependence on the plasma current. ($\chi_e \sim L_s$ does not help with the radial dependence of course, but it does give some current scaling, and a dependence on the local shear compatible with results of "current ramp" experiments). However, any strong inverse dependence of χ_e on L_n leads, for ordinary L-modes, to a stronger decrease in transport with increasing density than that observed (the density profiles tend to flatten at high density). Furthermore, it would imply worse confinement in peaked-density regimes, contrary to what is observed e.g. in the JET "PEP mode" (HUGON et al. (1992)).

A dependence $\chi_e \sim 1/L_T$, on the other hand, has the appealing feature of replacing (part of) the temperature dependence with a ∇T-dependence, which guarantees a degree of "profile resiliency", is compatible with low heat transport inside H-mode plasmas with strong edge temperature "pedestals", and yields fast heat pulse propagation. It may also help make gyro-Bohm-type models compatible with results of ρ_*-scaling experiments in JET (TARONI et al. (1993)).

Dissipative trapped electron modes have stronger dependencies on T than the pure gyro-reduced Bohm form, leading to too strong a degradation with power and even poorer radial profiles.

(ii) Models based on electro-magnetic fluctuations where the step size involves the collisionless skin depth introduce a favourable density dependence of thermal energy confinement, which is also present in the data. (This observation is worth emphasising because empirical L-mode scalings which are based on magnetic measurements of τ_E, including non-thermal contributions, do not show this density dependence).

On the other hand, such models often fail to predict the observed degradation of confinement with input power. Also a χ_e proportional to transit or bounce frequency will tend to have the wrong radial dependence and to yield the wrong scaling with current. Again, an inverse dependence on the shear length will help with radial dependence, but conflict with evidence from current ramp experiments. As an example, a suitable "mix of ingredients" seems to be present in Zhang and Mahajan's expression (31).

(iii) At first sight resistive fluid turbulence models would seem to be very promising: the resistivity η increases strongly towards the edge, β or the pressure gradient provide the degradation of confinement with power, and the predictions possess the correct shear dependence. Unfortunately, the magnitude of the predicted transport is often incorrect, as is in some cases the current scaling. Even the models that compare best with the experimental evidence, often leave something to be desired, e.g. Eq. (40) yields a density dependence at odds with observations. Equation (43a) represents the best all round performance.

(iv) A similar problem affects the best amongst the models for transport induced by magnetic islands (we exclude the "critical ∇T_e" model because it has been assessed in depth elsewhere, see REBUT et al. (1991)). Kadomtsev's Eq. (52) yields good radial profiles for χ_e (except near the very edge), and clearly provides a good local counterpart for the global Goldston scaling $\tau_{E,G} \sim \beta_p^{-1}$. It even provides theoretical support for a positive dependence of confinement on ion mass. However, just like the quoted global scaling, it cannot match the observed favourable dependence on the plasma density.

ACKNOWLEDGEMENTS

This work was undertaken under a JET Task Agreement as part of a joint collaboration between JET and AEA Technology, Fusion on comparing theories of anomalous transport with JET data and was funded by the United Kingdom Department of Trade and Industry and EURATOM. The authors wish to acknowledge the encouragement and support of D.F. Duechs and M. Keilhacker, useful discussions with J.G. Cordey and A. Taroni, as well as the contribution by G.P. Maddison in the early stages of this work, and the assistance of G. Corrigan and A. Galway in setting up and maintaining the FALCON code and data base used to analyse the local power balance of JET plasmas.

REFERENCES

BISHOP C.M., CONNOR J.W. (1990) Plas. Phys. Cont. Fus. **32** 203

CALLEN J.D., SHAING K.C. (1985) Phys. Fluids **28** 1845

CARRERA R., HAZELTINE R.D., KOTSCHENREUTHER M., (1986) Phys. Fluids **29** 899

CARRERAS B.A.,et al. (1983), Phys. Rev. Letters **50**, 503

CARRERAS B.A., DIAMOND, P.H. (1989) Phys. Fluids **B1** 1011

CARRERAS B.A., GARCIA L., DIAMOND, P.H. (1987) Phys. Fluids **30** 1388

CHEN L., CHENG C.Z. (1980) Phys. Fluids **23** 2242

CONNOR J.W. (1986) Nucl. Fus. **26** 517

CONNOR J.W. (1988) Plas. Phys. Contr. Fus. **30** 619

CONNOR J.W. (1993) Plas. Phys. Contr. Fus. **35** 757

CONNOR J.W., CHEN L. (1985) Phys. Fluids **28** 2207

CONNOR J.W., TAYLOR J.B. (1984) Phys. Fluids **27** 2676

CONNOR J.W., HASTIE R.J. (1993) Private Communication.

CONNOR J.W., et al. (1993), "An assessment of Theoretical Models based on Observations in the JET Tokamak - Part I: Ion Heat Transport due to ∇T_i - Instabilities", Plas. Phys. Contr. Fus. **35** (1993) 319.

CONNOR J.W., TAYLOR J.B., WILSON H.R. (1993), Phys. Rev. Lett. **70** 1803

DIAMOND P.H. et al. (1983) *Proceedings of the 9th International Conference on Plasma Physics and Controlled Thermonuclear Research* (Baltimore, 1982) Vol. 1, IAEA, Vienna, 259

DIAMOND P.H., CARRERAS.B.A (1987) Comments Plasma Phys. Contr. Fusion **10** 271.

DIAMOND P.H. et al. (1990) *Proceedings of the 13th International Conference on Plasma Physics and Controlled Thermonuclear Research* (Washington, 1990) Vol. 2, IAEA, Vienna, P.9.

DOMINGUEZ R.R., WALTZ R.E. (1987) Nucl. Fus. **27** 65

DRAKE, J.F., and ANTONSEN, T.M. (1985) Phys. Fluids **28** 544

GANG F.Y., DIAMOND P.H., ROSENBLUTH M.N. (1991) Phys. Fluids **B3** 68

GARBET X., MOURGES F., SAMAIN A. (1990) Plas. Phys Cont. Fus. **32** 131

GARCIA L. et al. (1985) Phys. Fluids **28** 2147

GUZDAR P. N. et al. (1986) Phys. Rev. Lett. **57** 2818

HAHM T.S. et al. (1987) Phys. Fluids **30** 1452

HAHM T.S., TANG W.M. (1991) Phys. Fluids **B3** 989

HASSAM A.B., (1980) Phys. Fluids **23** 38

HASSAM A.B., DRAKE J.F. (1983) Phys. Fluids **26** 133

HIRSHMAN S.P., MOLVIG K. (1979) Phys. Rev. Lett. **42** 648
HORTON W. (1976) Phys. Fluids **19** 711
HORTON W. (1985) Plas. Phys. Cont. Fus. **27** 937
HORTON W., HONG B.G., TANG W.M. (1988) Phys Fluids **31** 2971
HORTON W., CHOI D., YUSHMANOV P.N., PARAIL V.V. (1987) Plas. Phys. Cont. Fus. **29** 901
HUGON M., et al. (1992) Nucl. Fus. **32** 33
ITOH K., et al. (1993) Plas. Phys. Cont. Fus. **35** 543
KADOMTSEV B.B., (1991) Nucl. Fus. **31** 1301.
KAW P.K. (1982) Phys. Lett. **90A** 290
KESNER J. (1989) Nucl. Fus. **29** 1397
KIM D.E. et al. (1990) Phys. Fluids **B2** 547
KWON O.J., DIAMOND P.H., BIGLARI H. (1990) Phys. Fluids **B2** 291
KWON O.J., DIAMOND P.H., HAHM T.S. (1989) Phys. Fluids **B1** 2172
LEE Y.C. et al. (1987) Phys. Fluids **30** 1331
MANHEIMER W.M., ANTONSEN T.M. (1979) Phys. Fluids **22** 957
MANHEIMER W.M., et al. (1976) Phys. Rev. Lett. **37** 287
MIKHAILOVSKII A.B. (1976) JETP Lett. **23** 394
MOLVIG K., HIRSHMAN S.P., WHITSON J.C. (1979) Phys. Rev. Lett. **43** 582
OHKAWA T. (1978) Phys. Letter. **67A** 35
PARAIL V.V., POGUTSE O.P. (1980) JETP Lett. **32** 384; *Proceedings of the 8th International Conference on Plasma Physics and Controlled Nuclear Fusion Research* (Brussels, 1980) Vol 1, IAEA Vienna, p.67
PARAIL V.V, YUSHMANOV P.N. (1985) JETP Lett. **42** 343
PEARLSTEIN L.D., BERK H.L. (1969) Phys. Rev. Lett. **23** 220
PERKINS F.W. (1984) *'Proceedings of the 4th International Symposium on Heating in Toroidal Plasmas'* (ENEA, Rome, 1984) Vol. 2, p.977
REBUT P.H., HUGON M., (1991) Plas. Phys. Cont. Fus. **33** 1085.
REBUT P H., WATKINS M L., GAMBIER D J., AND BOUCHER D., (1991) Phys. Fluids **B3** 2209
RECHESTER A.B., ROSENBLUTH M.N. (1978) Phys. Rev. Lett. **40** 88
ROGISTER A. (1989) *Proceedings of the Cadarache Workshop on Electrostatic Turbulence*, 4-6 October 1989, EUR-CEA-FC-1381
ROGISTER A., HASSELBERG G., WAELBROEK F.G., WIELAND J. (1988) Nucl. Fus. **28** 1053
ROMANELLI F., TANG W.M., WHITE R.B. (1986) Nucl. Fus. **26** 1515
ROSS D.W., MAHAJAN S.M. (1978) Phys. Rev. Lett. **40** 324
ROZHANSKII V.A. (1981) JETP Lett. **34** 56

SAMAIN A., (1984) Plas. Phys. Cont. Fus. **26** 731
SIMILON P.L., DIAMOND P.H. (1984) Phys. Fluids **27** 916
SMOLYAKOV A.I. (1989) Sov. J. Plas. Phys. **15** 667.
SMOLYAKOV A.I., HIROSE A. (1993) Phys. Fluids **B5**, 663
TANG W.M. et al. (1975) Phys Rev. Lett. **35** 660
TANG W.M., (1986) Nucl. Fusion **26**, 1605.
TANG W.M., ROMANELLI F., BRIGUGLIO S. (1988) Phys. Fluids **31** 2951
TANG W.M. (1990) *Theory of Fusion Plasmas* edited by E. Sindoni, F. Troyon and J. Vaclavik (Varenna 27-31 August 1990), Editrice Compositori, Bologna 1990, p.31.
TARONI A., et al. (1993), JET Report JET-P(93) 37, to be published.
TAYLOR J.B. (1977) *Proceedings of the 6th International Conference on Plasma Physics and Controlled Thermonuclear Research* (Berchtesgaden, 1976) Vol. 2, IAEA, Vienna p.323
THAYER D.R., DIAMOND P.H. (1987) Phys. Fluids **30** 3724
TSANG K.T., CATTO P.J., WHITSON J.C., SMITH J. (1978) Phys. Rev. Lett. **40** 327
WALTZ R.E., et al. (1987) *'Proceedings of the 11th International Conference on Plasma Physics and Controlled Thermonuclear Research'* (Kyoto, 1986) Vol. 1, IAEA, Vienna, p.345.
WESSON J. (1987) *Tokamaks*, Oxford University Press
WHITE R.B., ROMANELLI F. (1989), Phys. Fluid **B 1** 977.
ZHANG Y.Z., MAHAJAN S.M. (1988) Comments on Plas. Phys. Cont. Fus. **11** 243

APPENDIX

We list here the definitions of all non-standard variables used in this paper and not explicitly defined in the text. All parameters are averaged over magnetic flux surfaces (for example the local inverse aspect ratio is $\varepsilon = \langle r \rangle / \langle R \rangle$). Units are SI with temperatures in eV.

flux surface coordinate	$\rho = \sqrt{\psi_n}$ ψ_n = normalized poloidal flux
temperature ratio	$\tau = T_e / T_i$
thermal velocity (species j)	
sound speed	$c_s = \tau^{1/2} v_{ti}$
gyroradii	$\rho_i = \sqrt{2} v_{ti} / (Z_i eB / m_i c)$ $\rho_s = \rho_i \tau^{1/2}$
profile scale lengths (a = n,T)	$L_a = -a / \nabla a \quad , \quad \varepsilon_a = L_a / R$ $\eta_e = L_{n_e} / L_{T_e}$
magnetic shear	$\hat{s} = \varepsilon R \ \nabla q / q$
shear length	$L_s = Rq / \hat{s}$
electron plasma frequency	$\omega_{pe} = \left(4\pi n_e e^2 / m_e\right)^{1/2} \simeq 56.4\, n_e{}^{1/2}$
collision frequencies	$\nu_{ei} = 2.9 \cdot 10^{-12} n_e Z_{eff} \Lambda_c T_e{}^{-3/2}$ $\nu_{ii} = 4.8 \cdot 10^{-14} n_i Z_i{}^4 \Lambda_c m_i{}^{-1/2} T_i{}^{-3/2}$ with $\Lambda_c = 31 - 0.5 \log(n_e) + \log(T_e)$ $\nu_{eff} = \nu_{ei} / \varepsilon$

mode frequency	ω
bounce frequency (species j)	$\omega_{bj} = \varepsilon^{1/2} v_{tj} / qR$
magnetic drift frequencies	$\omega_{di} = -k_\theta \rho_i v_{ti} / \left(R\sqrt{2}\right),\ \omega_{de} = -\tau\omega_{di}$
transit frequency (species j)	$\omega_{tj} = v_{tj} / qR$
diamagnetic frequencies	$\omega_{*i} = -k_\theta \rho_i v_{ti} / \left(L_n\sqrt{2}\right),\ \omega_{*e} = -\tau\omega_{*i}$
collisionality parameter	$\nu_{*j} = \nu_{ji} / \left(\varepsilon\omega_{bj}\right)$
ratio thermal/magnetic pressure	$\beta = 2\mu_o p / B^2$
S number	$S = \tau_R / \tau_A$
resistive diffusion time	$\tau_R = \varepsilon^2 R^2 \mu_o / \eta$
poloidal Alfvén time	$\tau_A = \left(\mu_o n_i m_i\right)^{1/2} Rq / B$
	with $\eta =$ electrical resistivity $\mu_o = 4\pi \cdot 10^{-7}$ henry / m

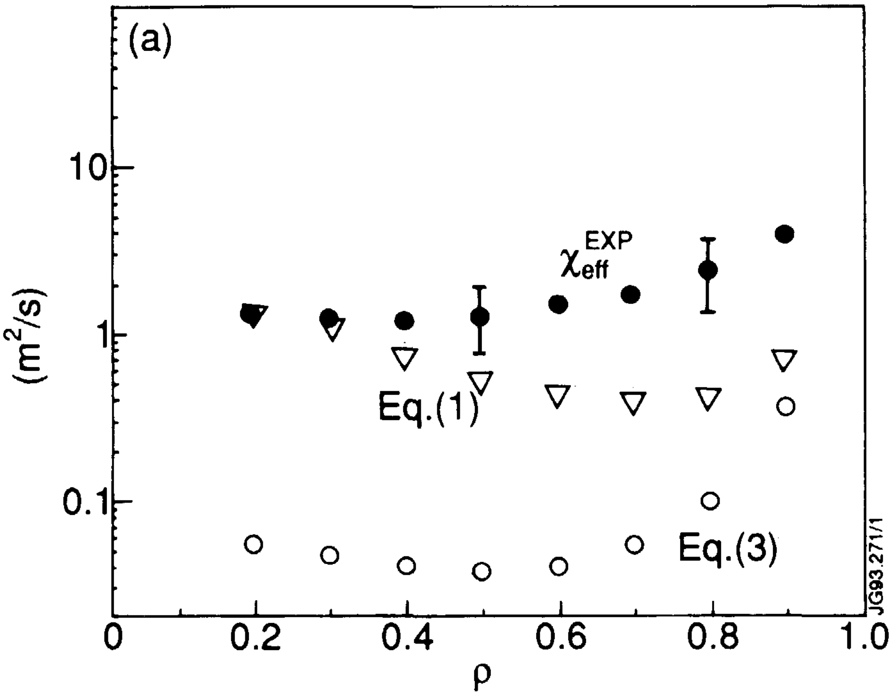

Figure 1. **(a)** Local effective thermal diffusivity for a typical JET L-mode plasma compared with theoretical models Eq. (1) by HIRSHMAN and MOLVIG (1979) and Eq. (3) by MOLVIG et al. (1979). Details of experimental profiles and power balance for this discharge (pulse #19699, $B_t = 3T$, $I_p = 3MA$, $\langle n_e \rangle \simeq 3 \cdot 10^{19} m^{-3}$, $P_{NBI} + P_{ICRF} \simeq 10MW$) can be found in Figure 1 of CONNOR et al. (1993).

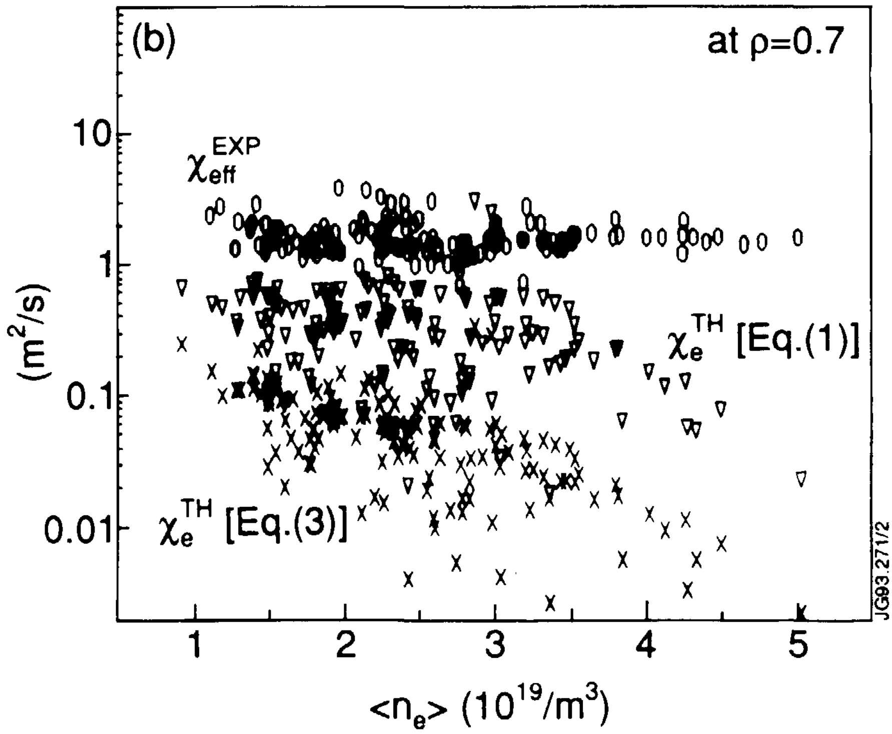

(b) Experimental and predicted thermal diffusivity at normalized minor radius ρ = 0.7 versus average plasma density for a set of approximately 100 sawtooth-free JET (mostly L-mode) discharges, at various levels of plasma current, toroidal magnetic field and auxiliary input power.

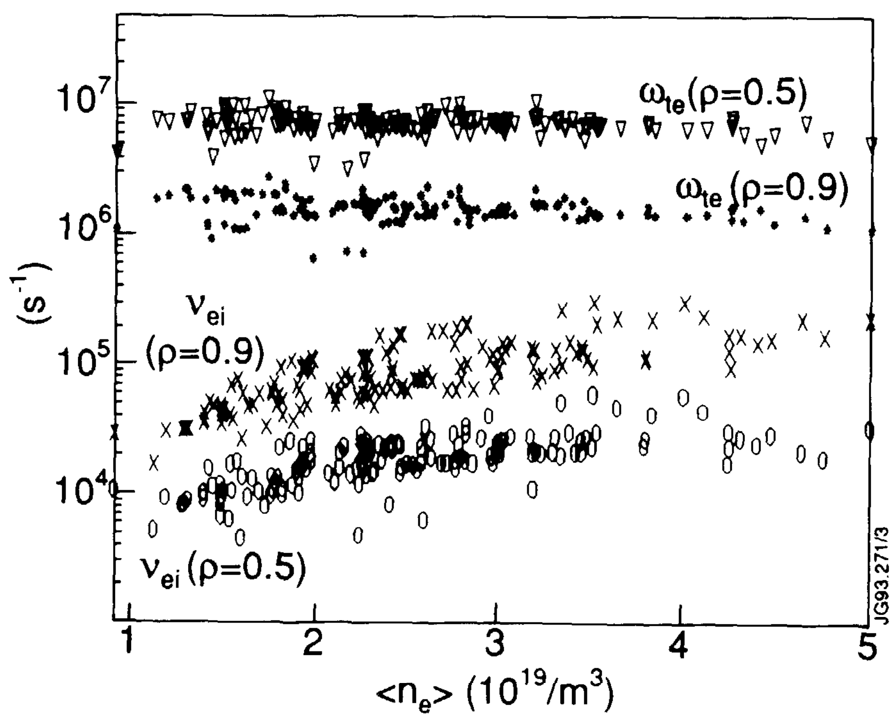

Figure 2. Electron transit frequency and electron-ion collision frequency at different radial positions, for the same set of data used in Figure 1b.

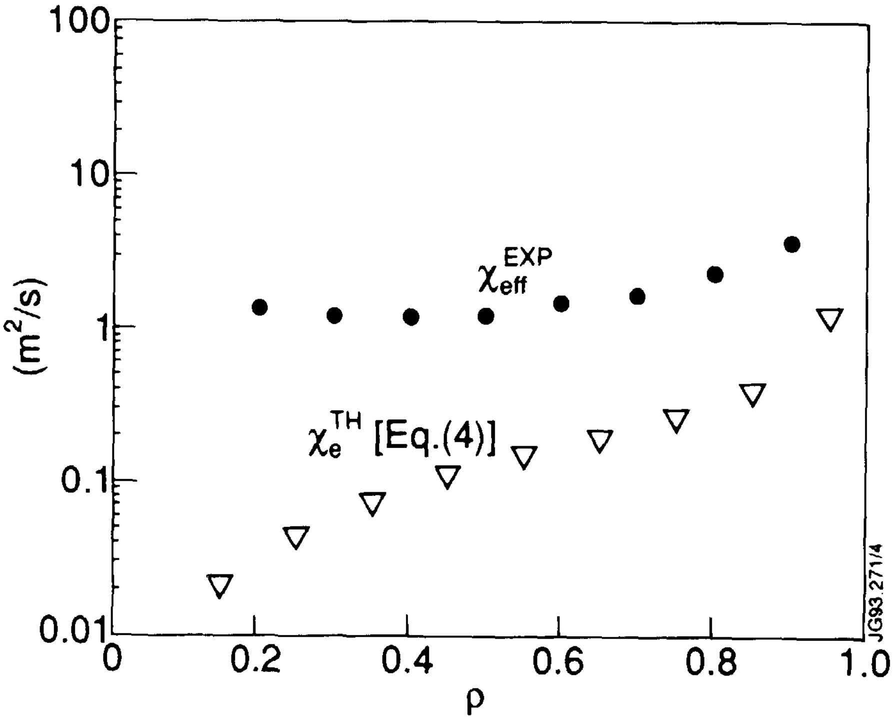

Figure 3. Comparison between the measured thermal diffusivity and that predicted in the collisionless regime, Eq. (4), by WALTZ et al. (1987), for the same plasma conditions as in Figure 1a.

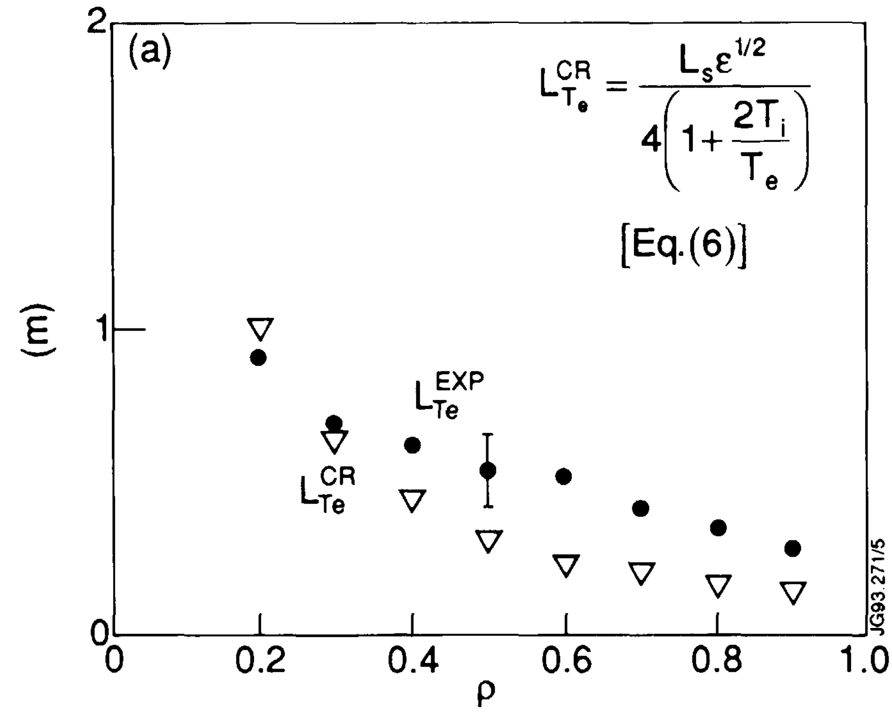

Figure 4. (a) Radial variation of the temperature scale length L_{Te}, Eq. (6), expected by MANHEIMER et al. (1976) at marginal stability, compared with the measured one for the JET discharge of Figure 1a.

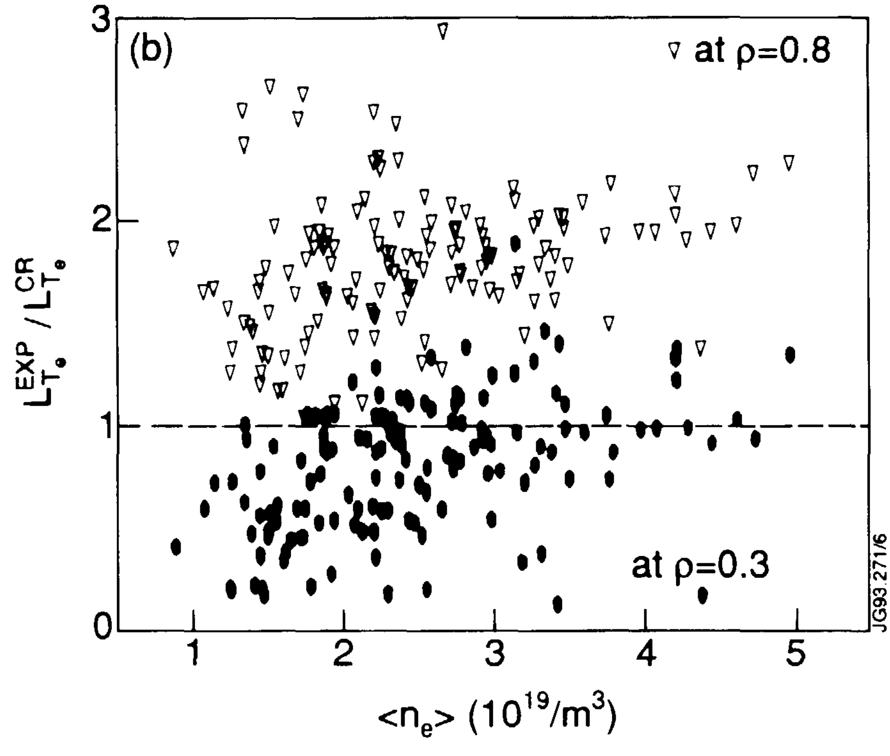

(b) Ratio between measured and critical L_{Te} at different radial locations, plotted as a function of plasma density for the data set of Figure 1b.

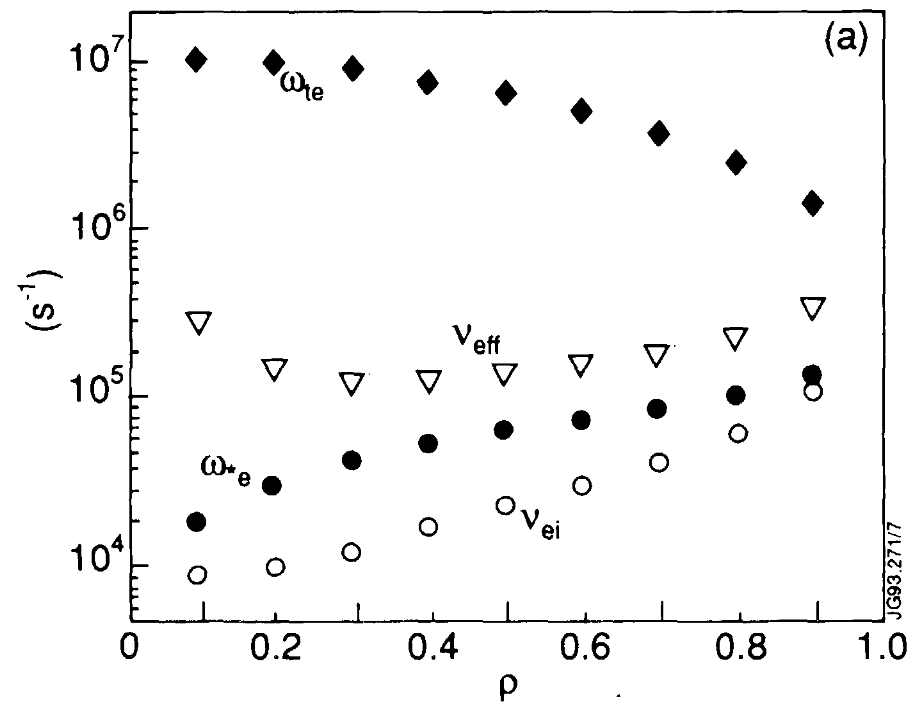

Figure 5. (a) Radial variation of the characteristic frequencies that determine the transition from collisionless to dissipative regime according to DOMINGUEZ and WALTZ (1987), for the JET discharge of Figure 1a.

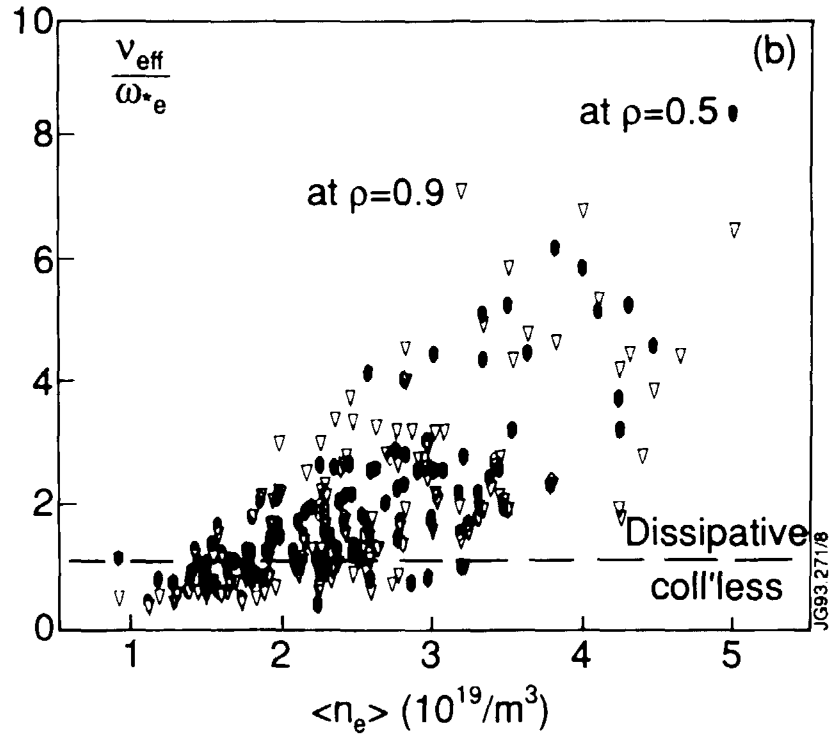

(b) Ratio of effective collision frequency to electron diamagnetic frequency at two different radii, as a function of plasma density, for the data set of Figure 1b.

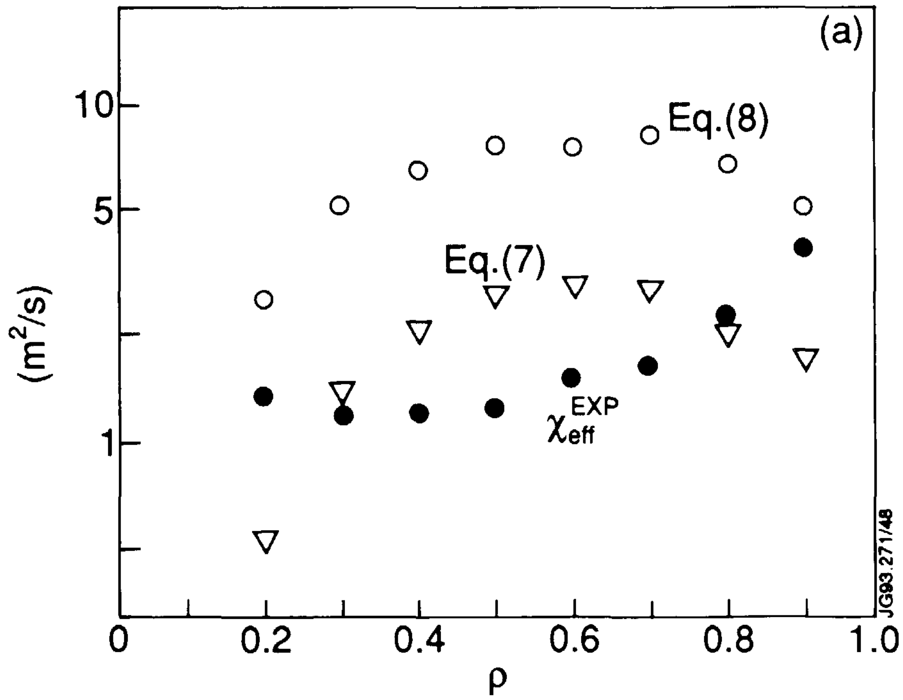

Figure 6. (a) Thermal diffusivities for trapped electron modes according to DOMINGUEZ and WALTZ (1987) and ROMANELLI et al. (1986), compared with the measured profile of Figure 1a.

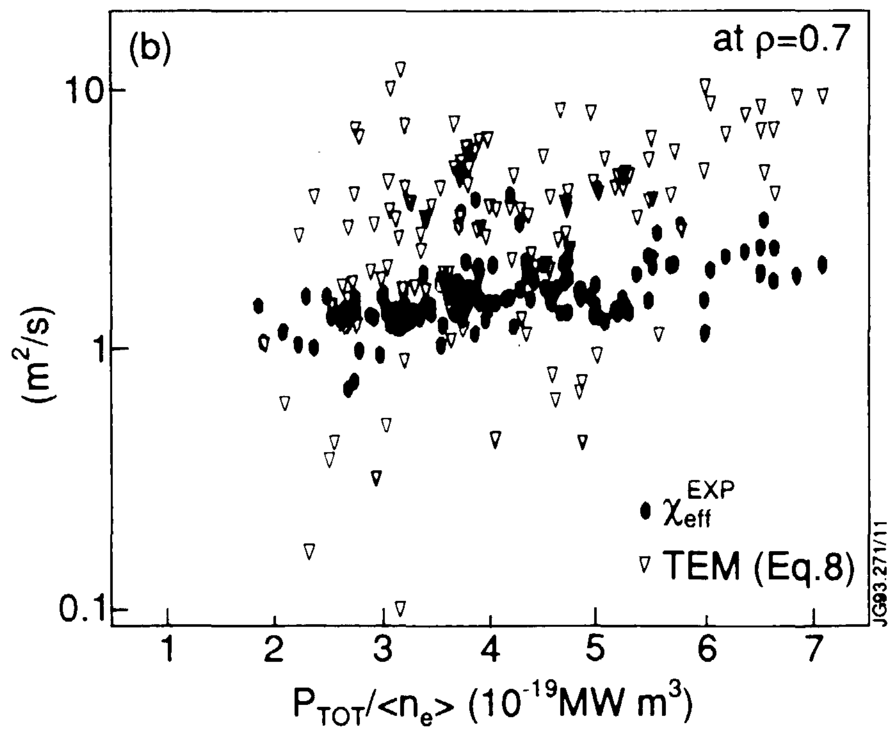

(b) Thermal diffusivity predicted by Eq. (7) and measured value, both at ρ = 0.7, plotted versus the average input power per particle for the data set of Figure 1b.

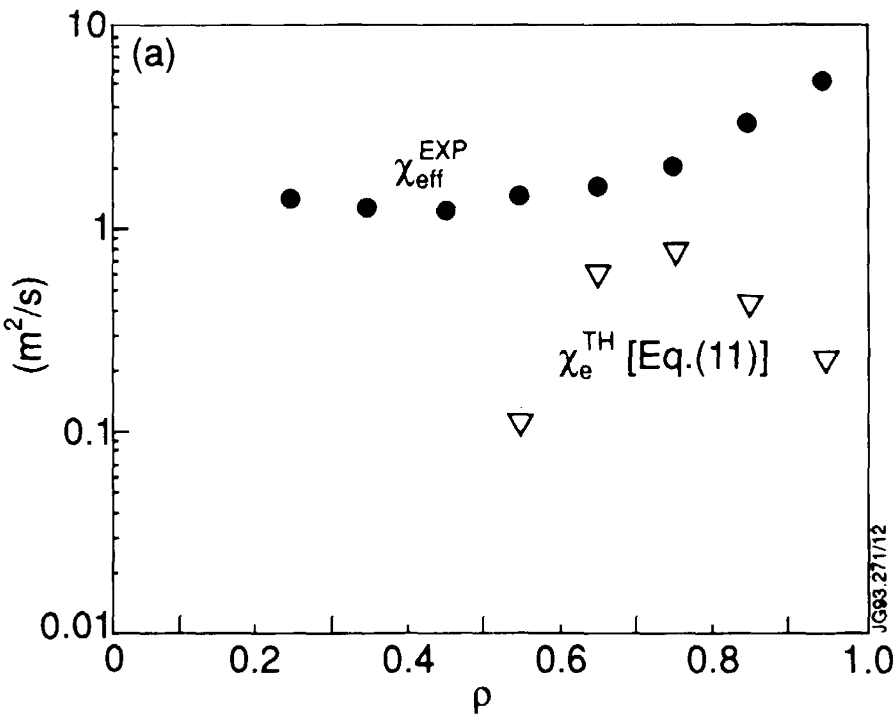

Figure 7. **(a)** Snapshot radial comparison between the weak turbulence electron thermal diffusivity of Eq. (11) by GANG et al. (1991) and that inferred from measurements (data as in Figure 1a.).

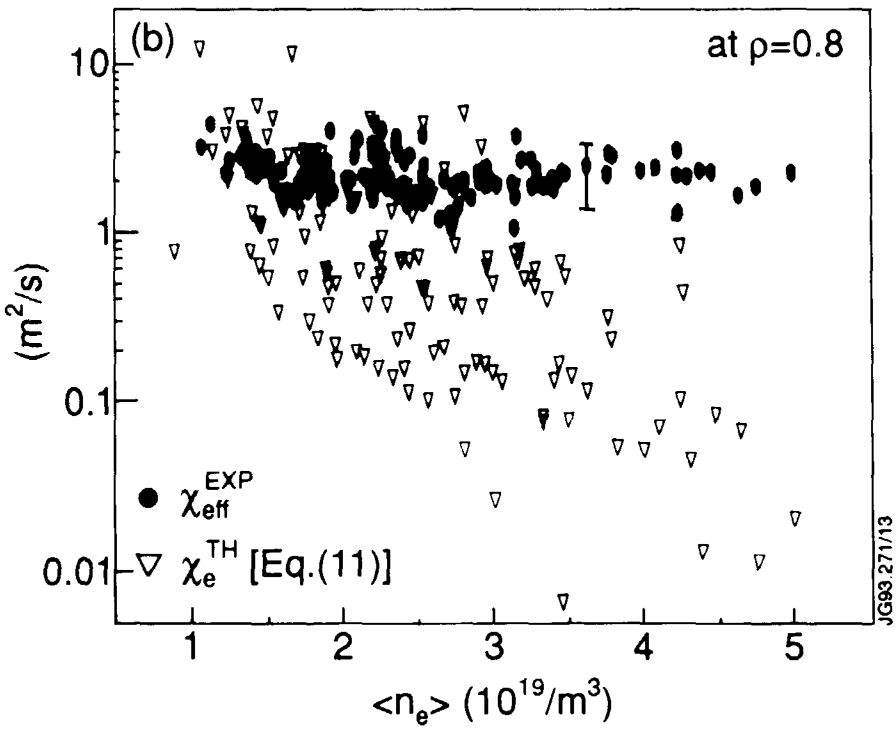

(b) Density dependence of predicted and measured transport coefficients in the outer plasma (data as in Fig 1b.).

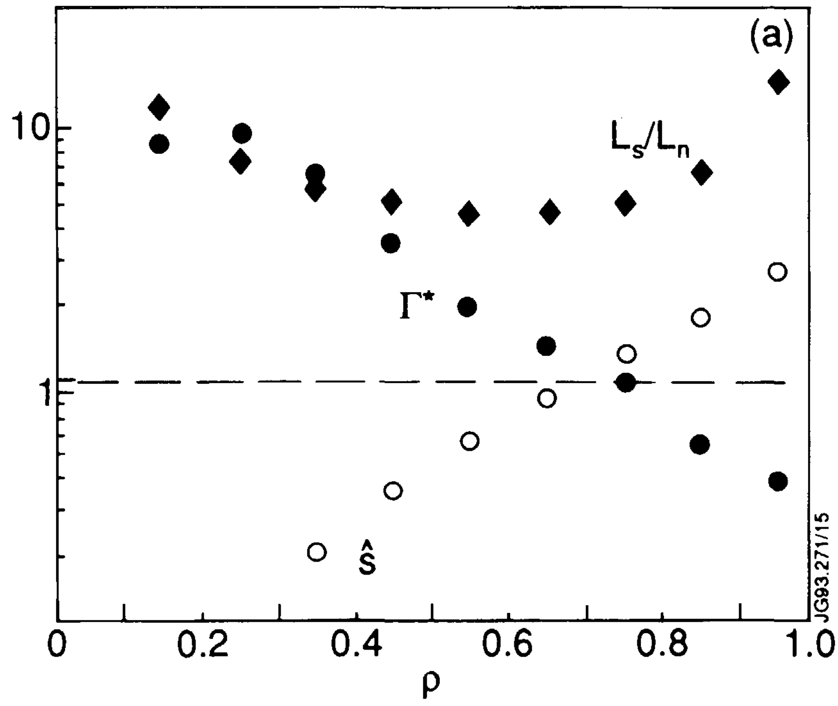

Figure 8. (a) Radial variation of the marginal stability parameter Γ^* of ROGISTER (1989), Eq. (13), here with $\lambda/(k_\theta \rho_s) \simeq 1$, for representative JET L-mode data. Magnetic shear and the ratio between shear and density scale length are also shown.

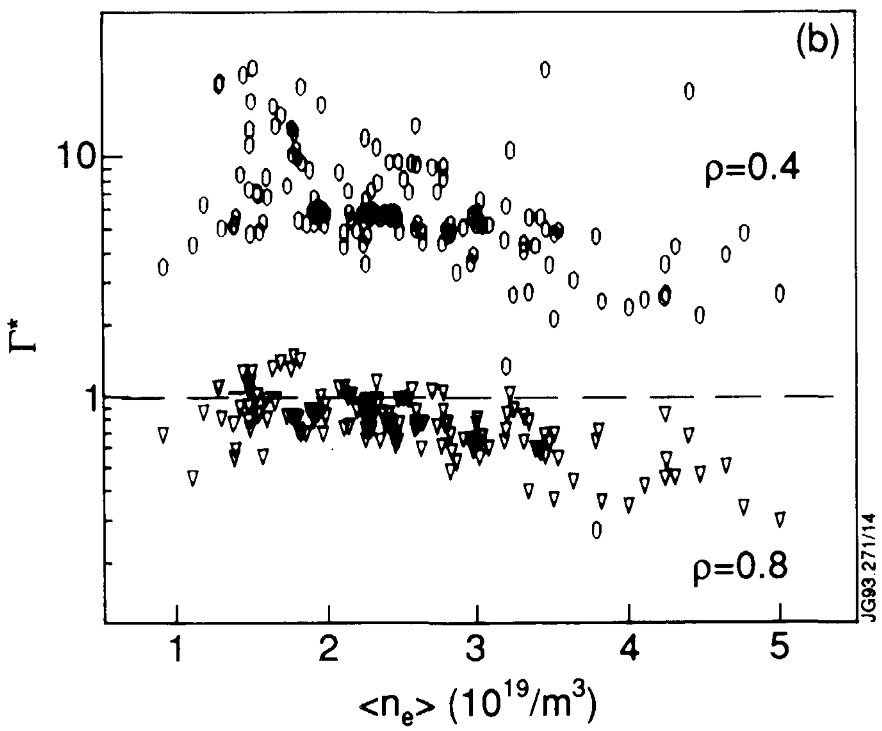

(b) Variation in Γ^* at different radial locations with the plasma density for the data set of Figure 1b.

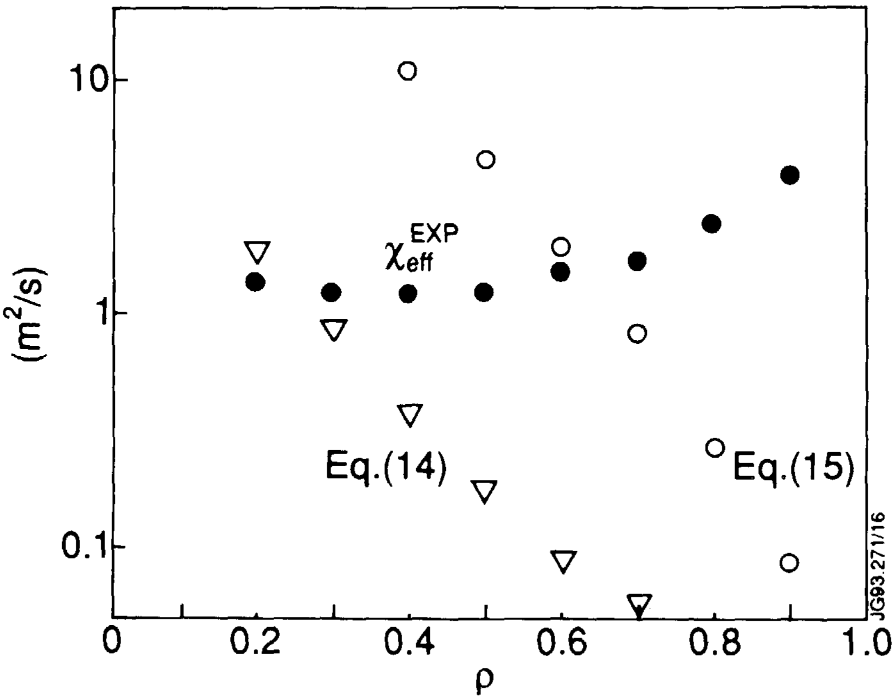

Figure 9. Comparison between the measured χ_{eff} and the theoretical χ_e predicted by SIMILON and DIAMOND (1984) for trapped and untrapped electrons.

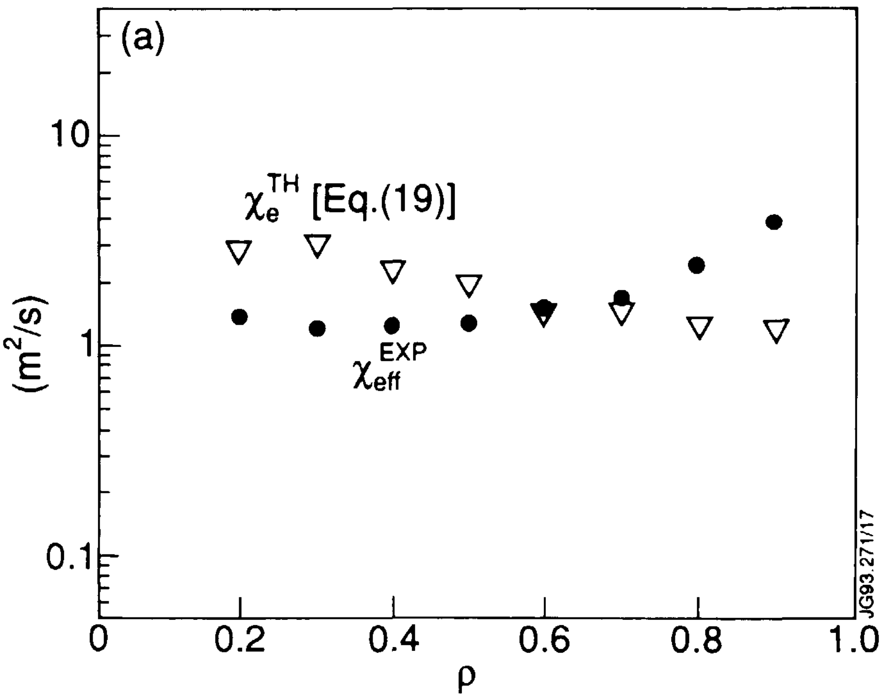

Figure 10 . (a) Thermal diffusivity profile from measurements (as in Figure 1a) and from Eq. (19) by KAW (1982).

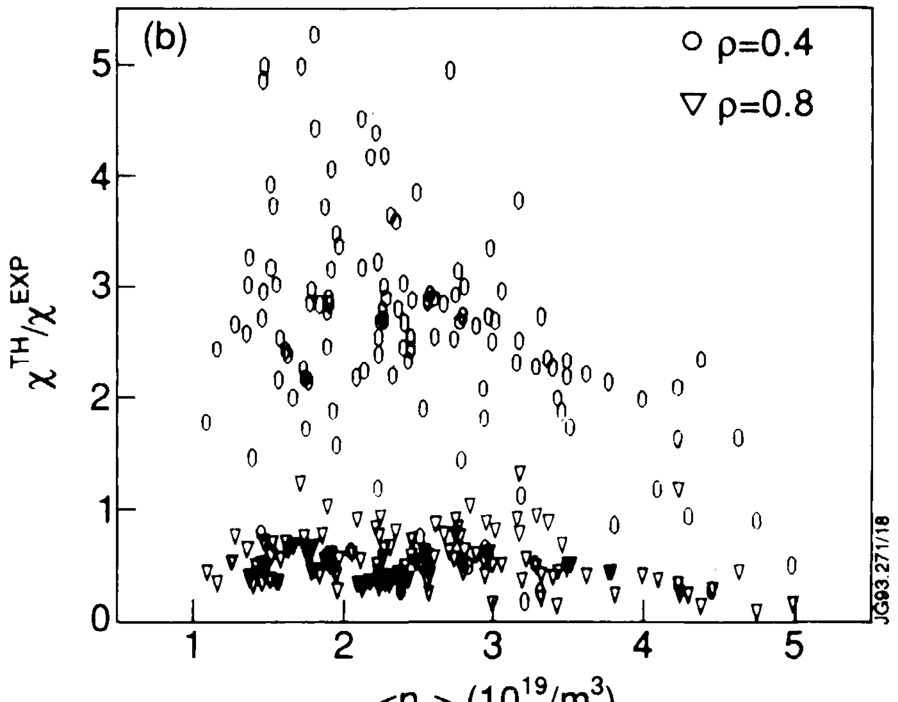

(b) Variation with density of the ratio between predicted and experimental thermal diffusivity at two radial positions.

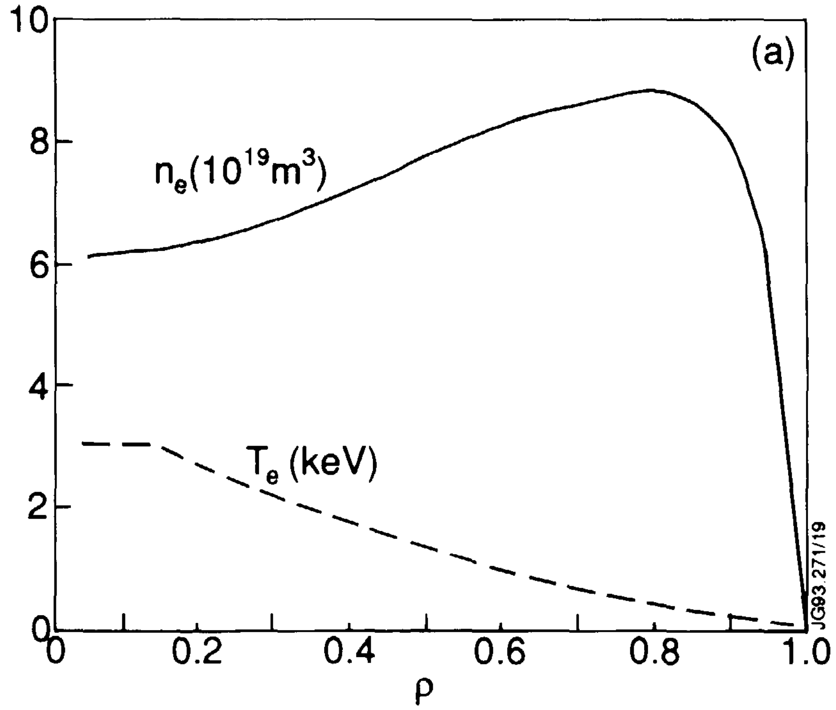

Figure 11. (a) Density and temperature profile measured in a high-density JET H-mode discharge (pulse # 21024 - $B_t = 2.2T$, $I_p = 3.1MA$, double-null X-point, $P_{NBI} \simeq 7.5MW$).

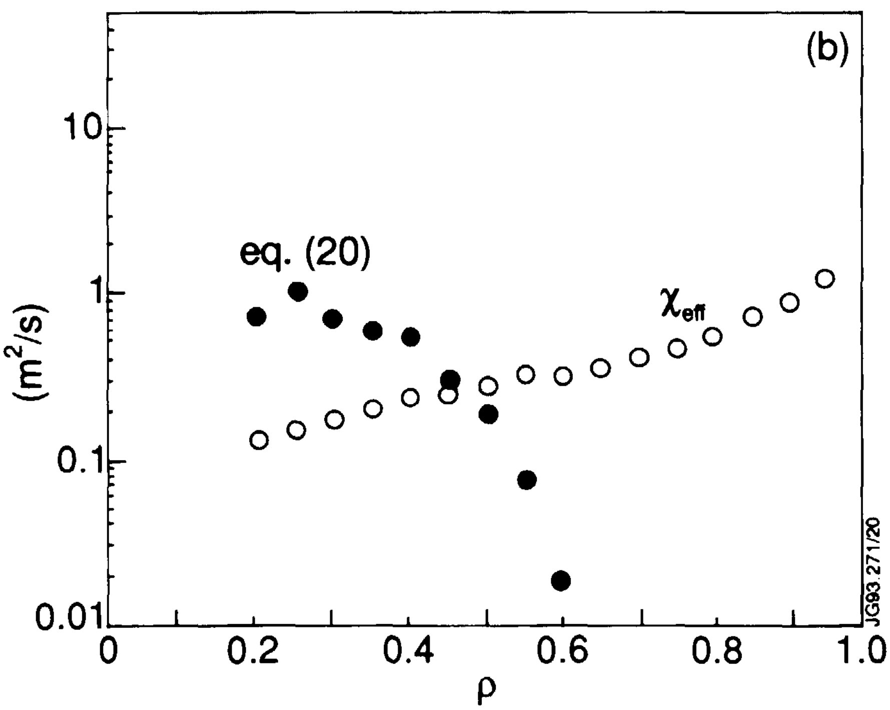

(b) Effective χ inferred from experimental data for the discharge of Figure 11a, compared with the prediction of Eq. (20) by BISHOP and CONNOR (1990).

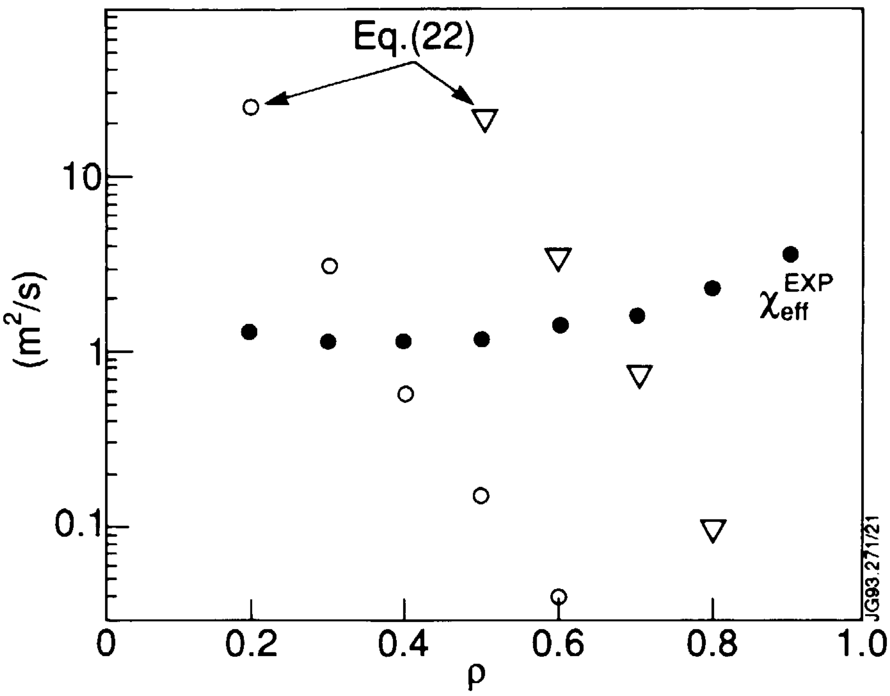

Figure 12. Upper and lower limit on a theoretical χ_e obtained using results by MIKHAILOVSKII (1976) and DIAMOND et al. (1990), compared with the measured χ_{eff} for the case of Figure 1a.

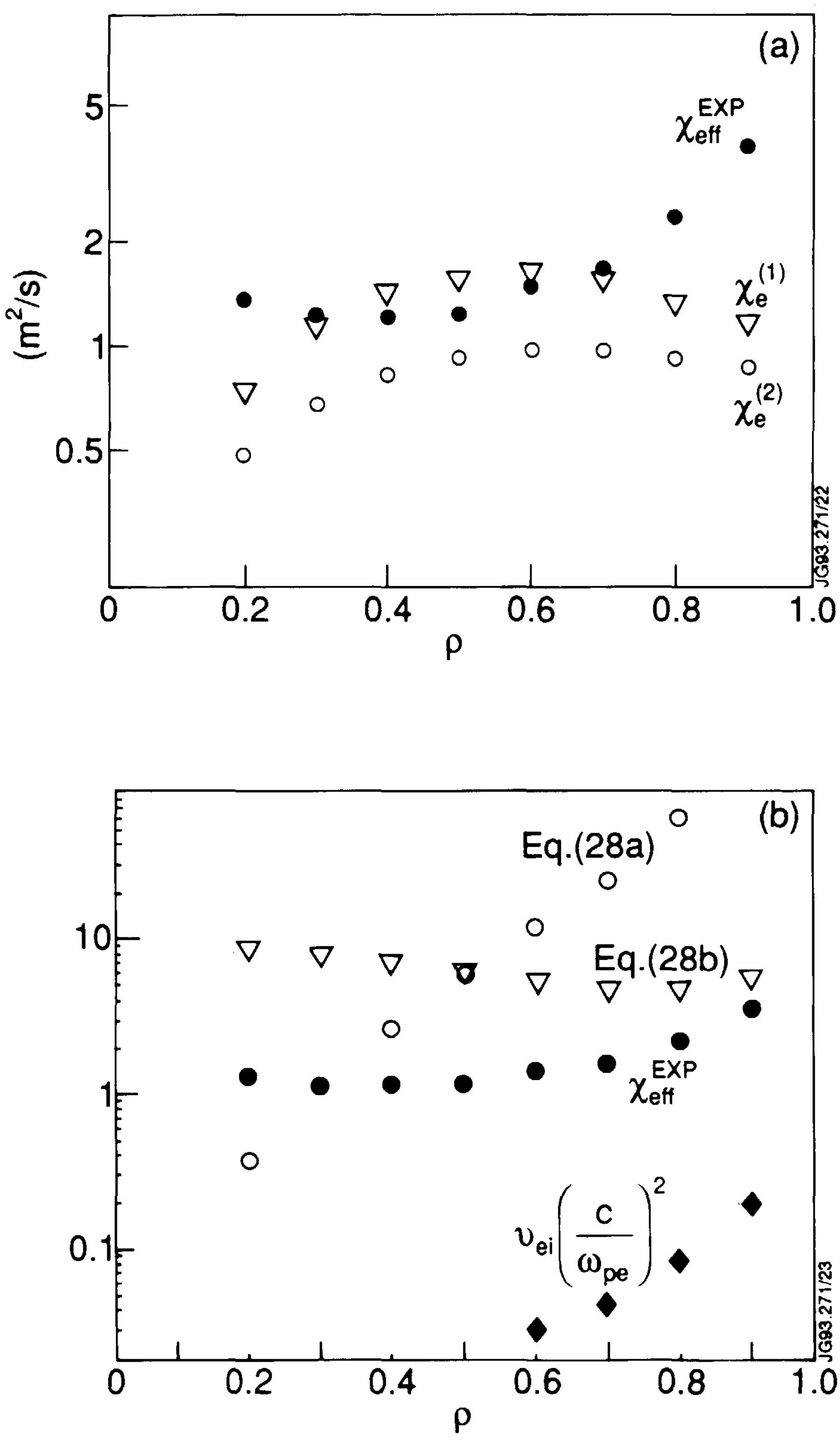

Figure 13. Snapshot comparison between the experimental thermal diffusivity of Figure 1a and **a)** the collisionless transport coefficients of HORTON(1985) and PARAIL and YUSHMANOV (1985), **not** including the shear dependence of Eq. (26), and **b)** the collisional expressions of KIM et al. (1990) and CONNOR and HASTIE (1993).

L-mode plasmas at 3MA
$9<P_{AUX}$ (MW)<11

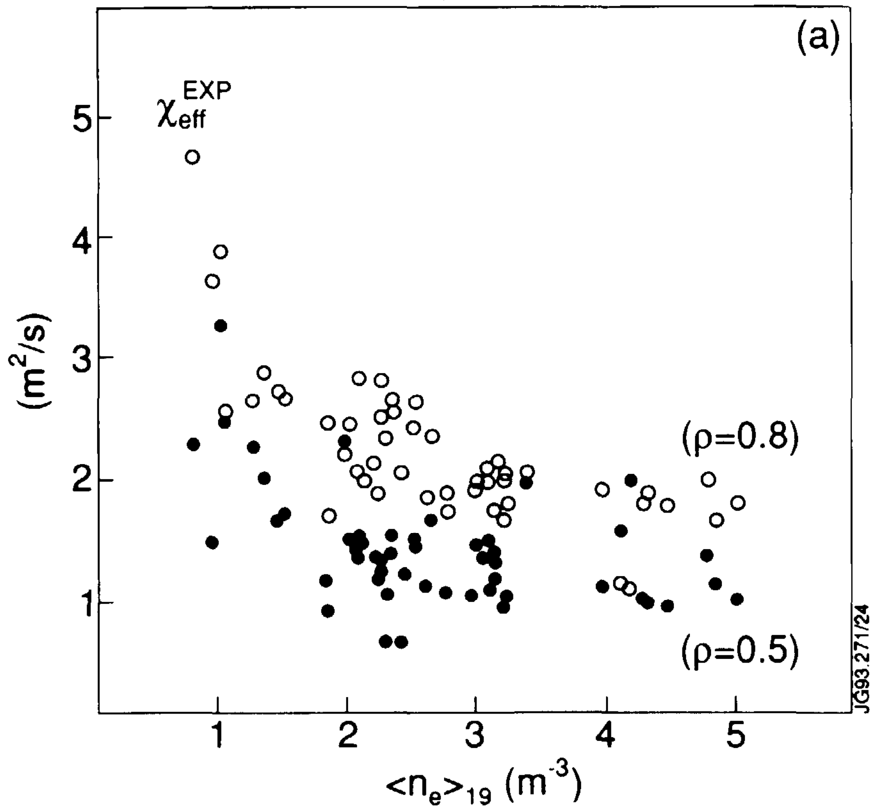

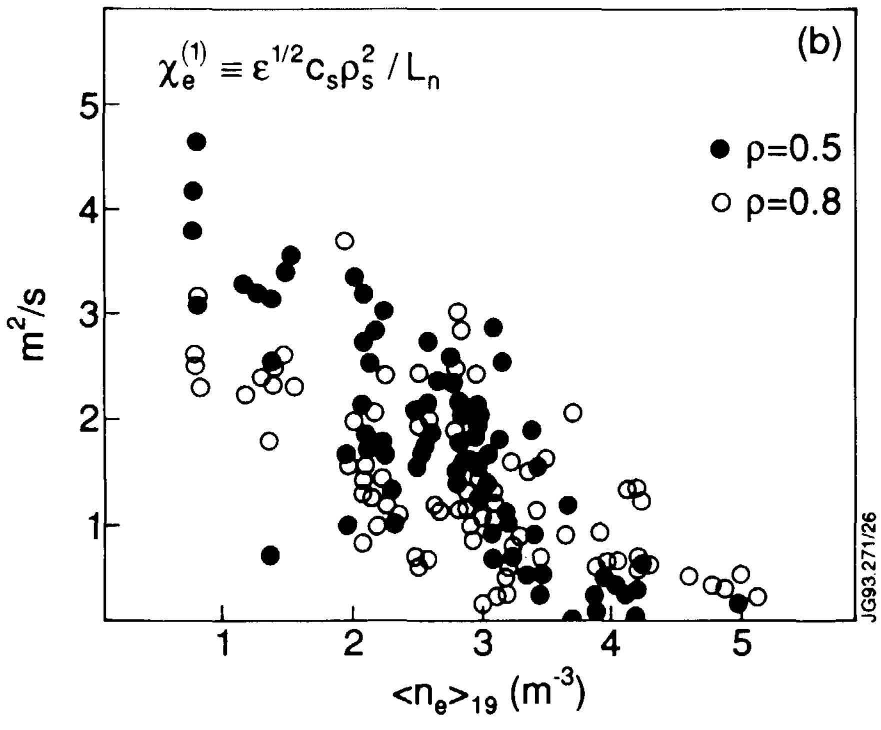

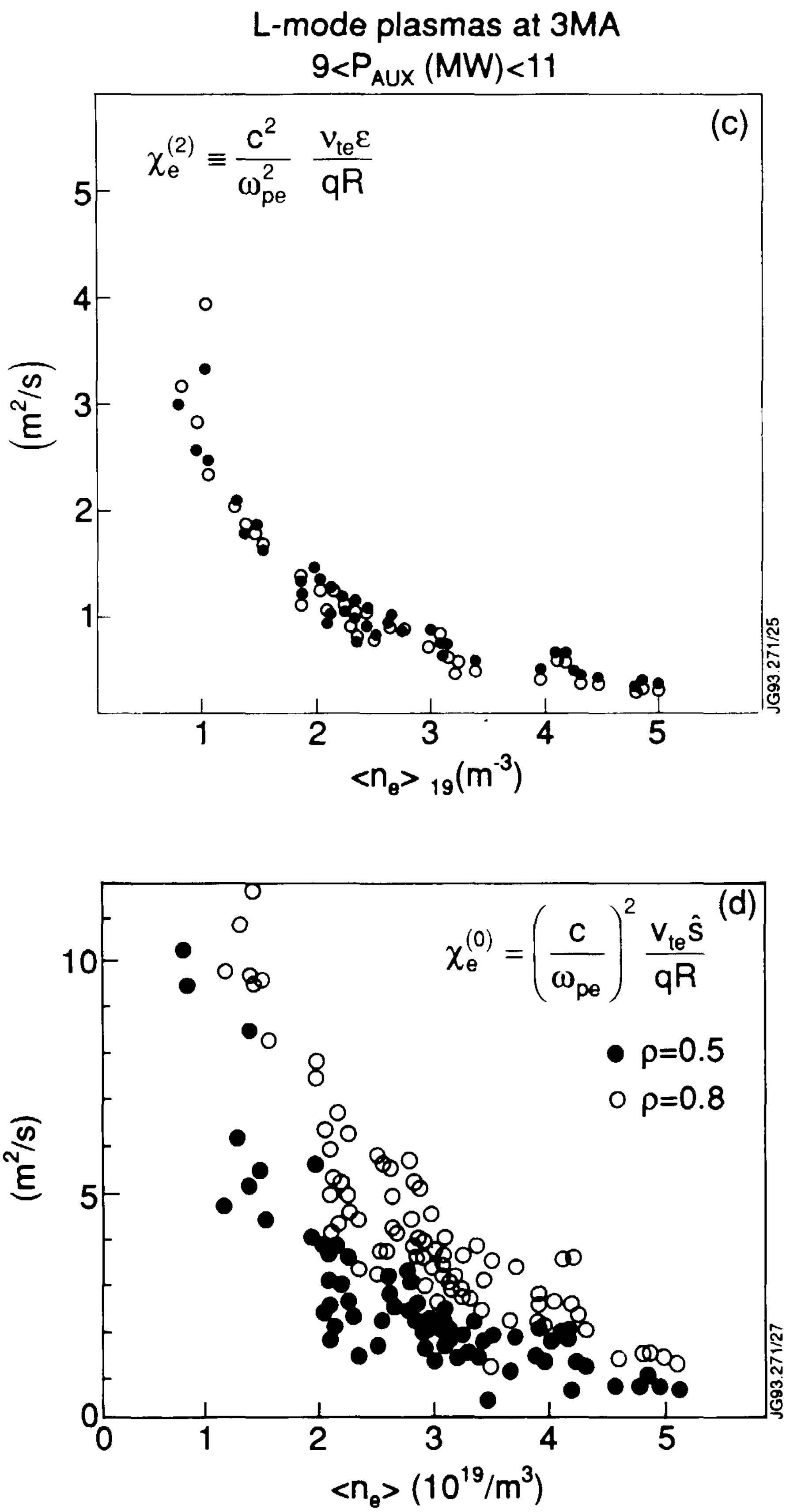

Figure 14. Density dependence of local energy transport: **a)** measured one-fluid heat diffusivity compared with predictions by **b)** Eq. (23) **c)** Eq. (24) and **d)** Eq. (29). The data correspond to JET limiter discharges at 3MA in deuterium, with auxiliary power $P_{AUX} = 10 \pm 1$ MW.

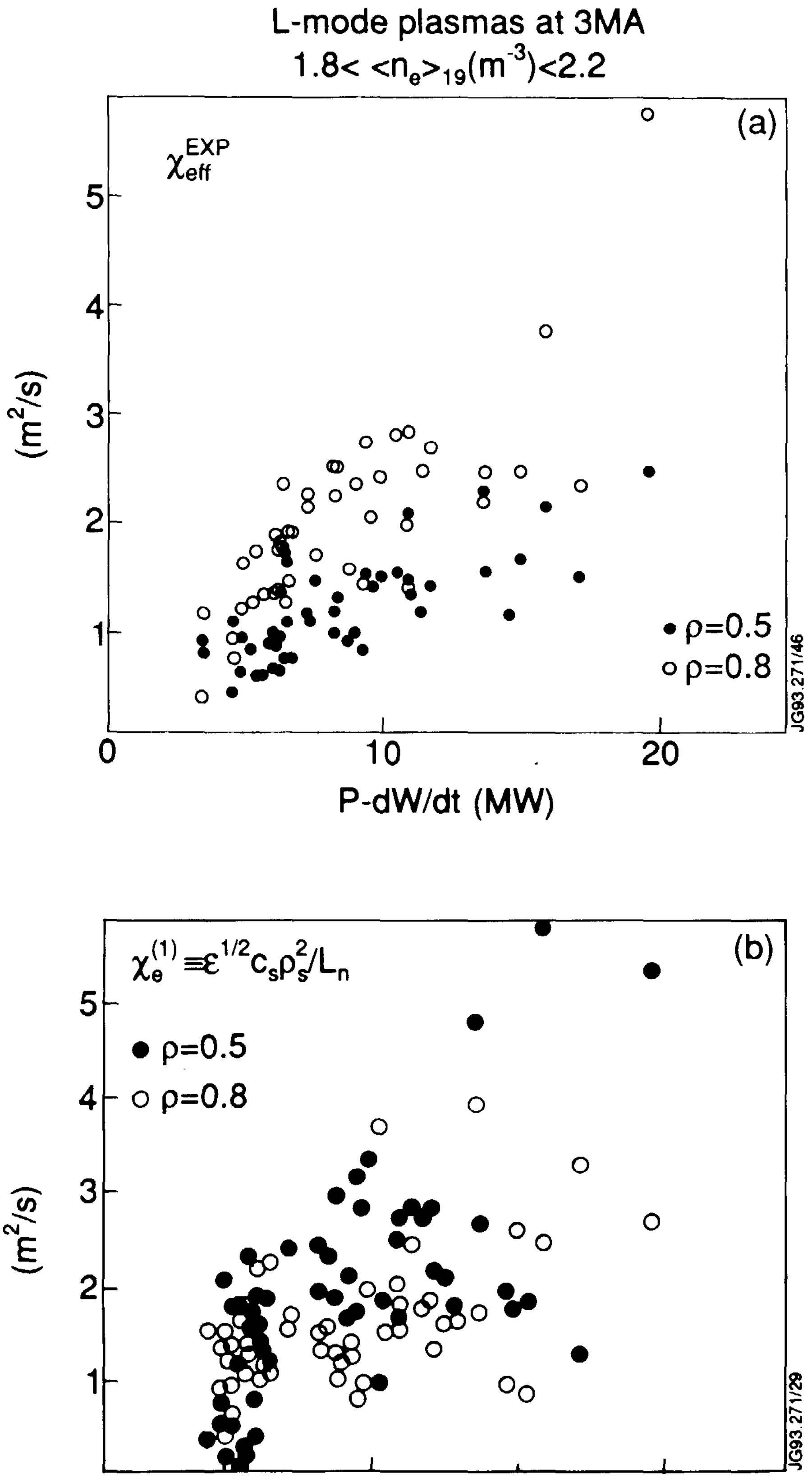

L-mode plasmas at 3MA
1.8< <n_e>_19(m^-3)<2.2
(a)
χ_eff^EXP
(m²/s)
● ρ=0.5
○ ρ=0.8
JG93.271/46
P-dW/dt (MW)
(b)
χ_e^(1) ≡ε^1/2 c_s ρ_s^2/L_n
● ρ=0.5
○ ρ=0.8
(m²/s)
JG93.271/29
P-dW/dt (MW)

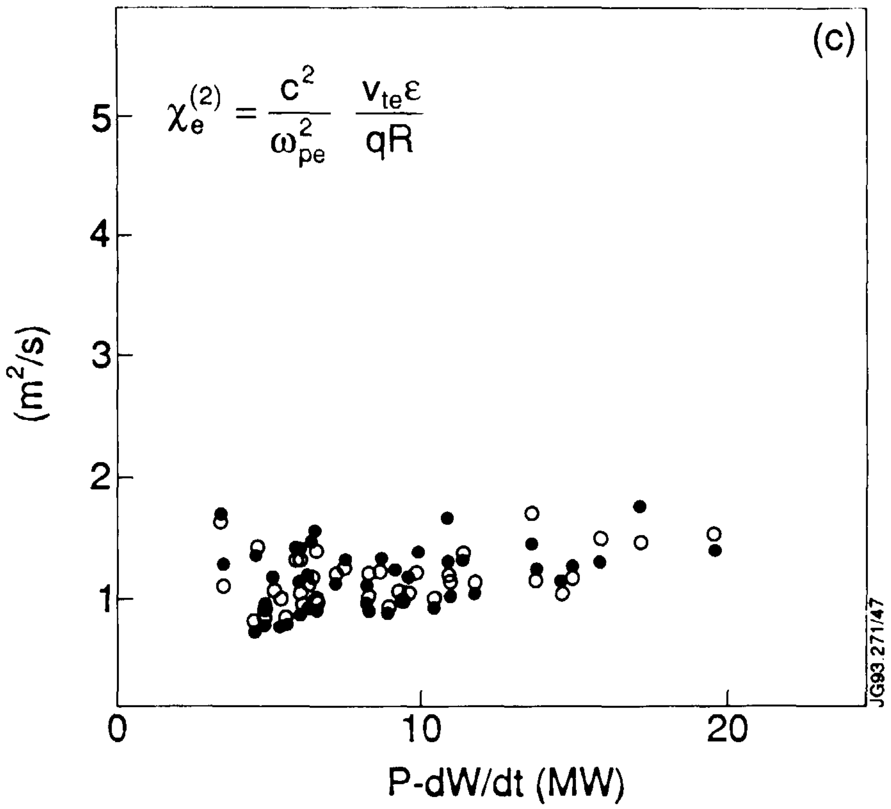

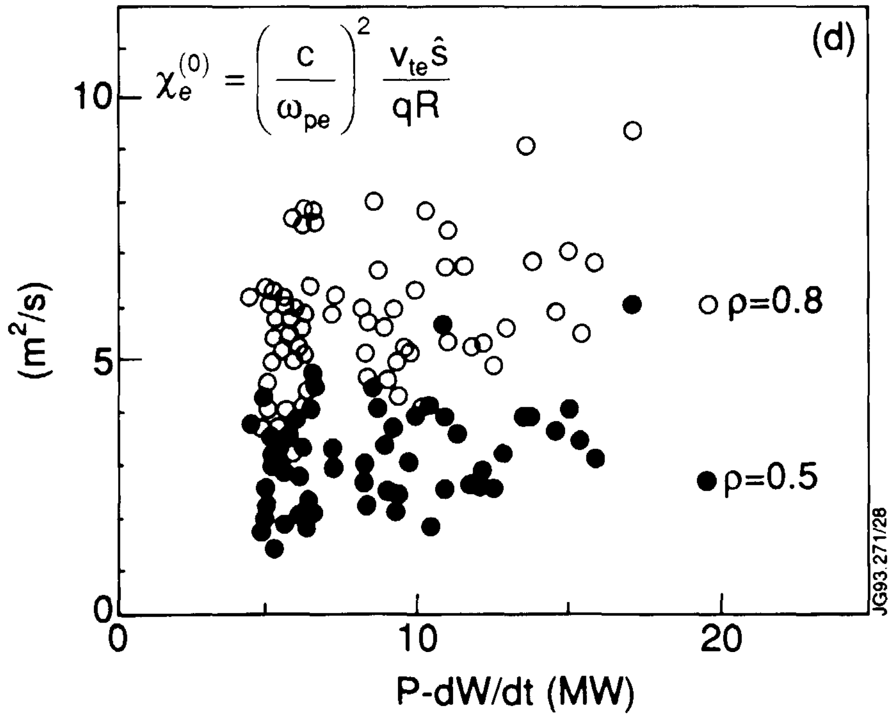

Figure 15. Dependence of local energy transport on input power at constant density (i.e. on plasma temperature). (**a, b, c, d**) are as in Figure **14.** The data correspond to JET limiter discharges at 3MA in deuterium, with average electron density $\langle n_e \rangle = (2.0 \pm 0.2)\cdot 10^{19}m^{-3}$.

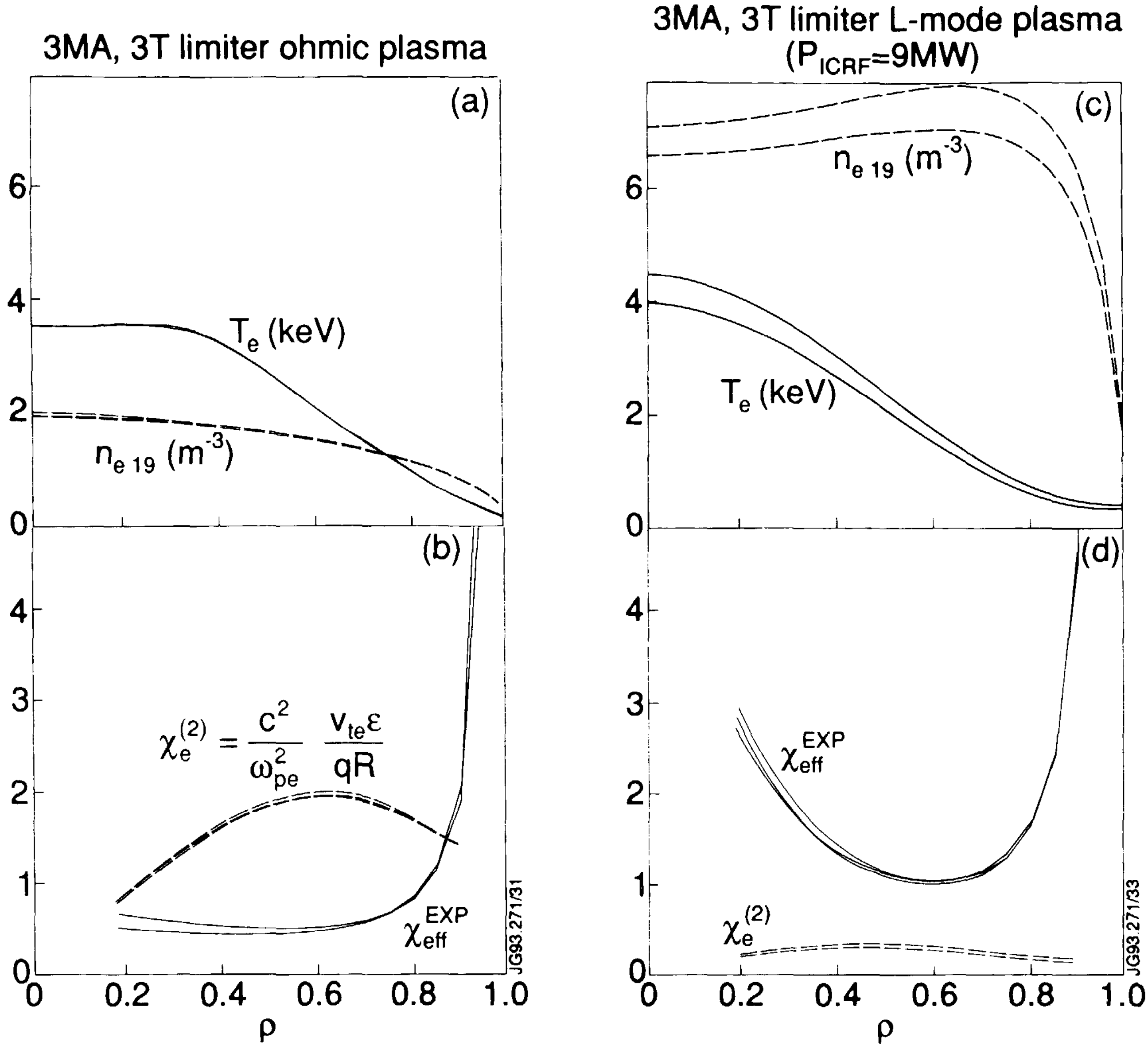

Figure 16. Ohmic and auxiliary-heated conditions may correspond to approximately the same temperature in a tokamak, if the density increases sufficiently in the L-regime. Figures (**a**) and (**c**) illustrate such a case from JET. It can be seen from (**b**) and (**d**) that $\chi_e^{(2)}$ varies in the opposite way to the measured χ_{eff}.

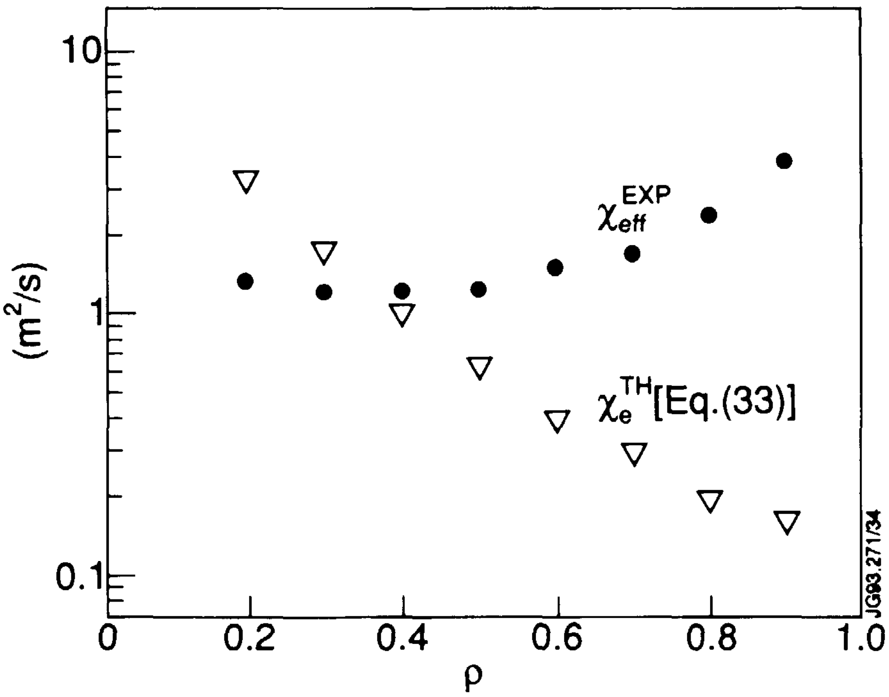

Figure 17. Transport predicted by the short wavelength mode theory of HORTON et al. (1988) compared with χ_{eff}^{EXP} of Figure 1a.

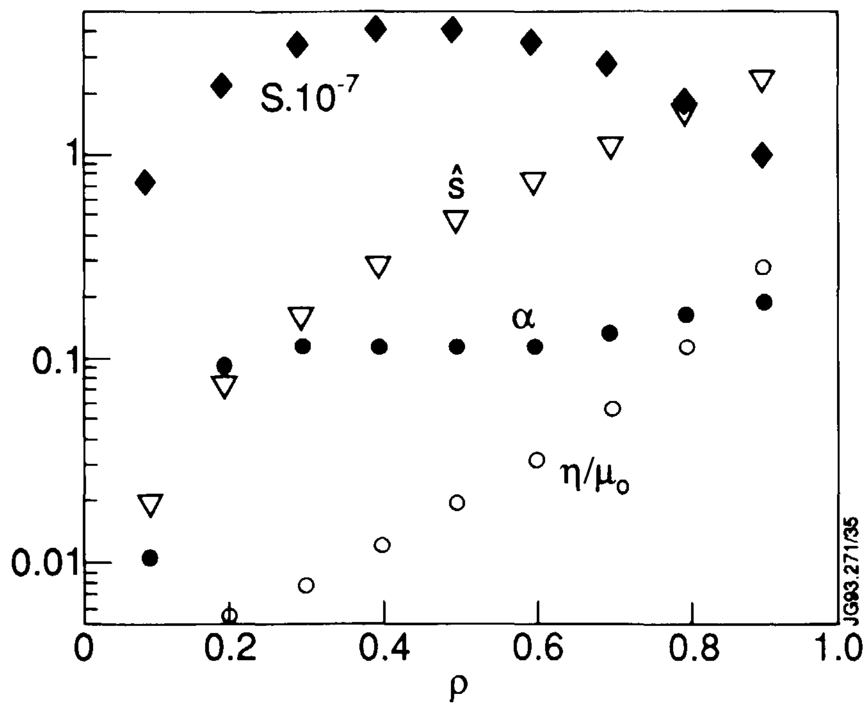

Figure 18. Radial profiles of parameters relevant to resistive fluid turbulence theories, based on typical JET L-mode data (see Figure 1 of CONNOR et al. (1993)). S is the ratio of resistive diffusion time to poloidal Alfvén time, $\hat{s}$ is the magnetic shear, α is the normalised pressure gradient of Eq. (36), η / μ_0 is the leading term in the diffusion coefficient of Eq. (35).

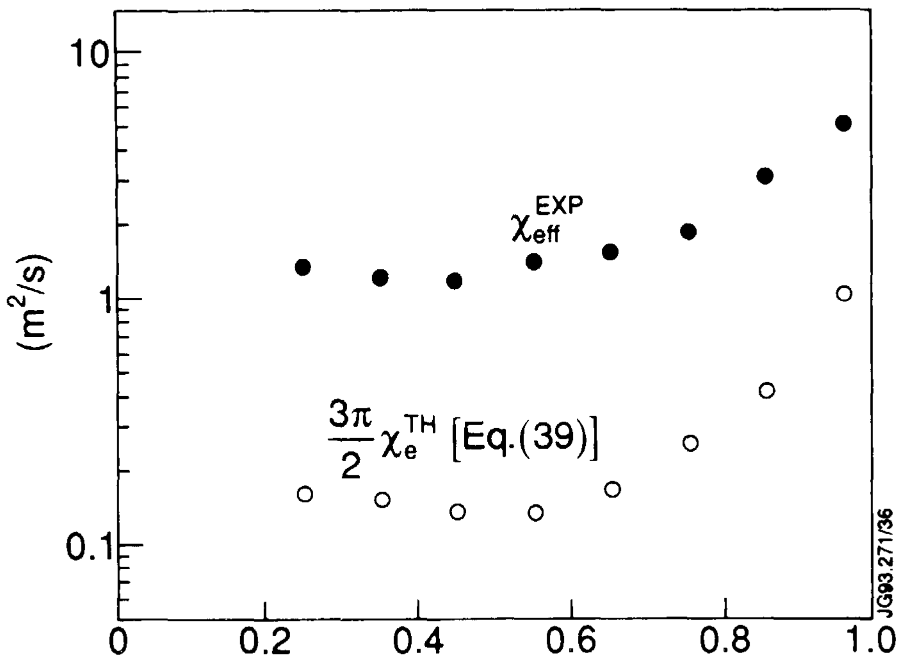

Figure 19. Transport coefficient based on the resistive interchange mode theory of CARRERAS et al. (1987), here with $g_0 = 1$, $m_0 = 3$, compared with χ_{eff}^{EXP} of Figure 1a.

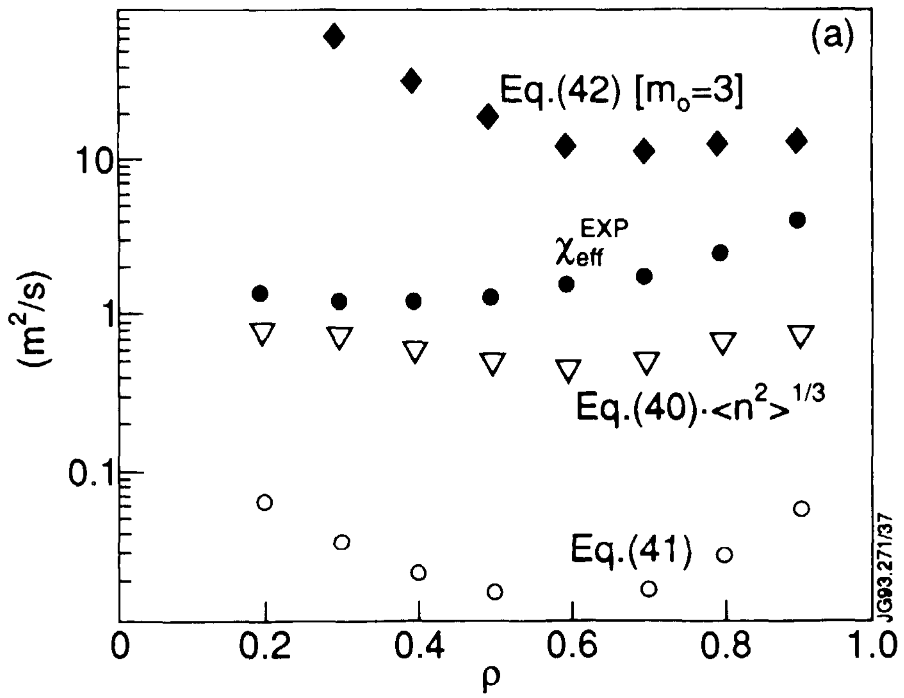

Figure 20. (a) As Figure 19, but using the work of CARRERAS and DIAMOND (1989) (without assumptions on the toroidal wavenumber) and of KWON et al. (1990) (assuming $m_0 = 3$).

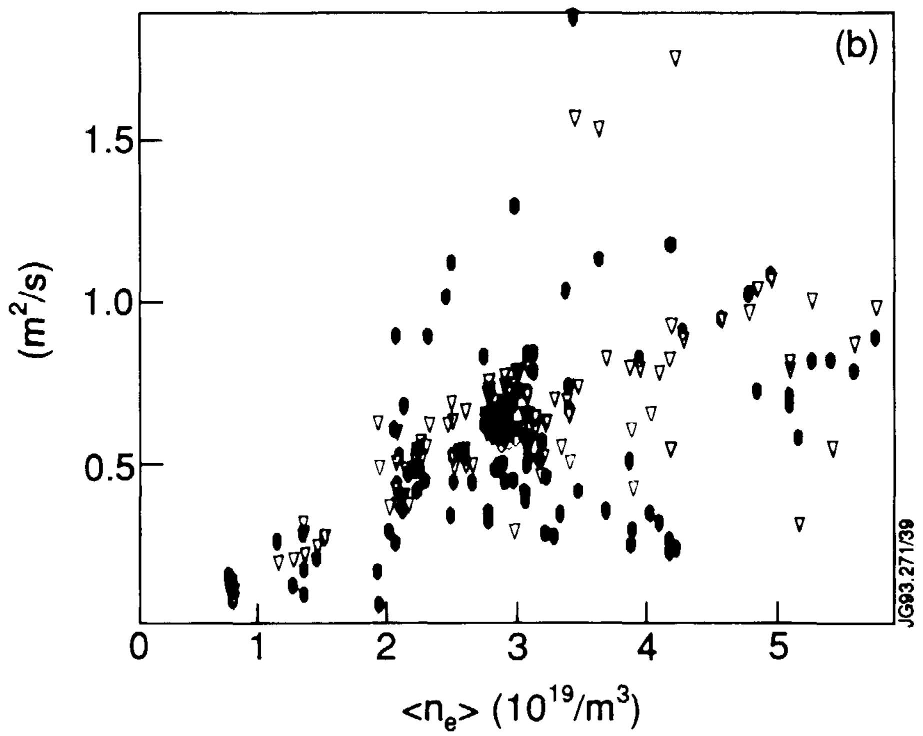

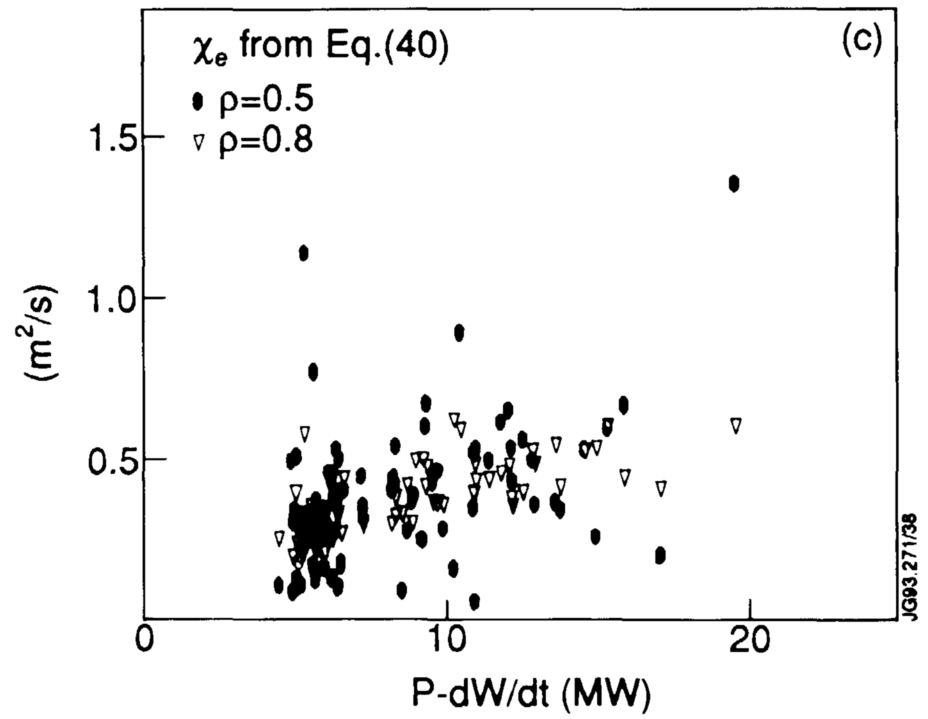

(b/c) Variation of χ_e^{TH} from Eq. (40) with plasma density/temperature, to be compared with the experimental data in Figures **14a** and **15a**.

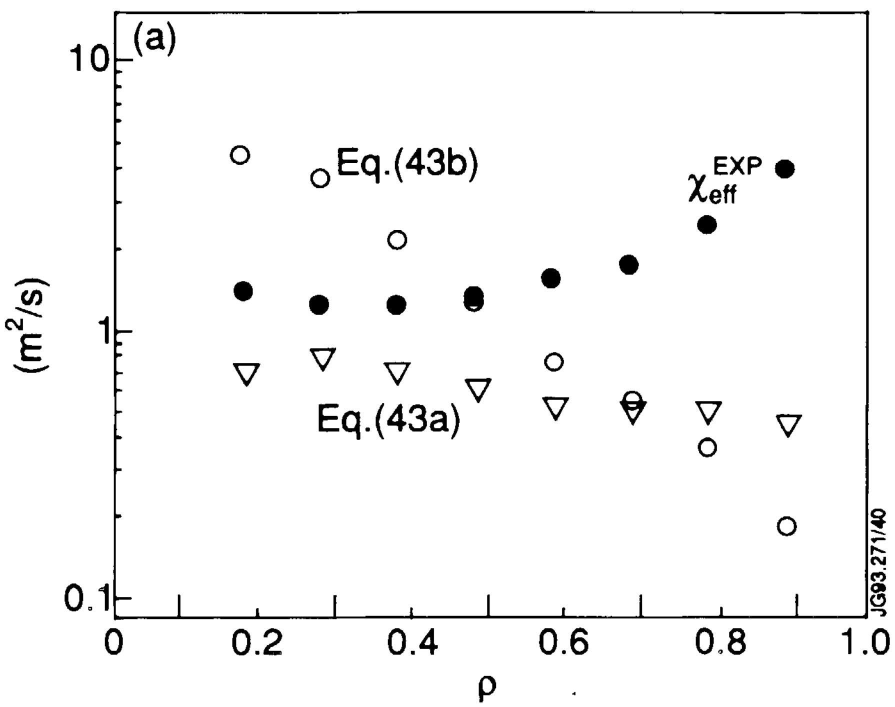

Figure 21. (a) Magnitude and radial variation of χ_e predicted by CONNOR (1993), compared with the measured transport coefficient.

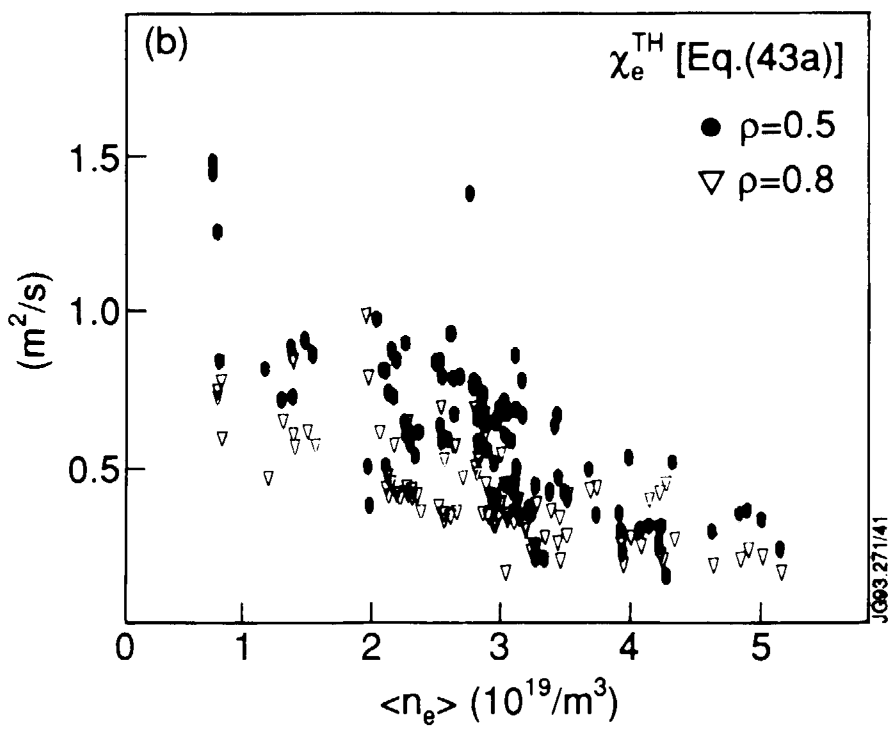

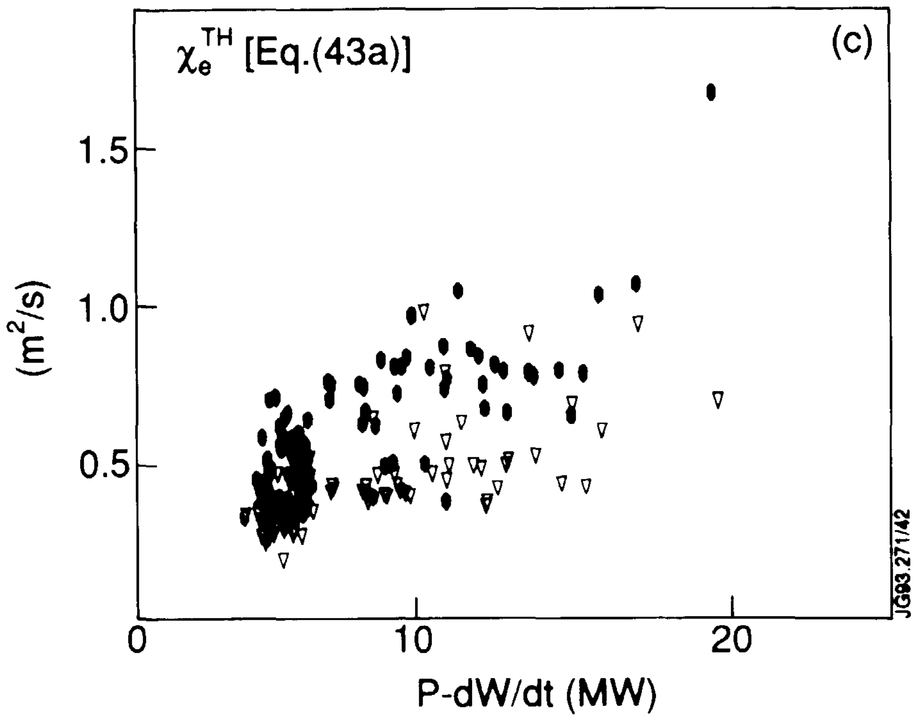

(b/c) Variation of χ_e^{TH} from Eq. (43a) with plasma density/temperature, to be compared with the experimental data in Figures **14a/15a**.

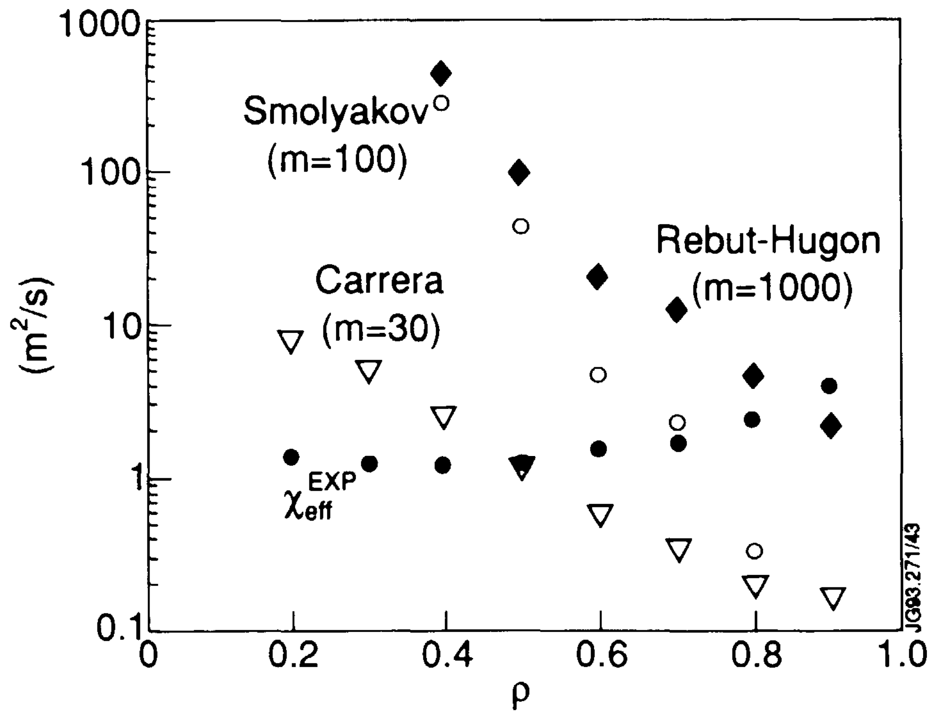

Figure 22. Theoretical heat diffusivities evaluated using the prescriptions for the magnetic island width given by CARRERA et al. (1986), SMOLYAKOV (1989) and REBUT and HUGON (1991).

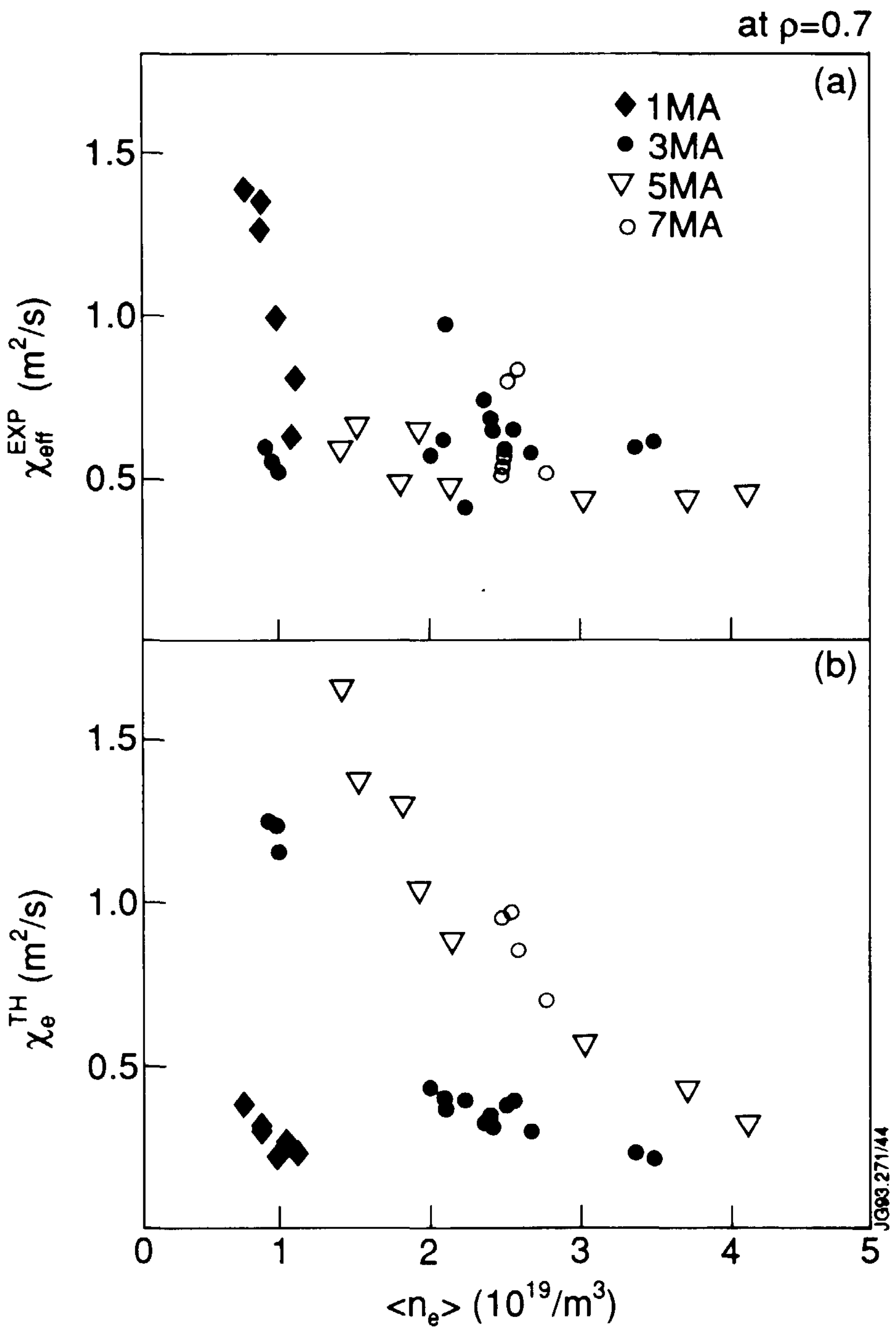

Figure 23. The "slanted island" model by KADOMTSEV (1991) in the limit of weak island overlap, Eq. (51), is used to estimate the heat transport to be expected at low heating power levels: **a)** measured thermal diffusivity in JET Ohmic discharges (for different values of the plasma current, and at a radius well outside the sawtooth region) as a function of the plasma density. **b)** corresponding χ_e^{TH} predicted by Eq. (51).

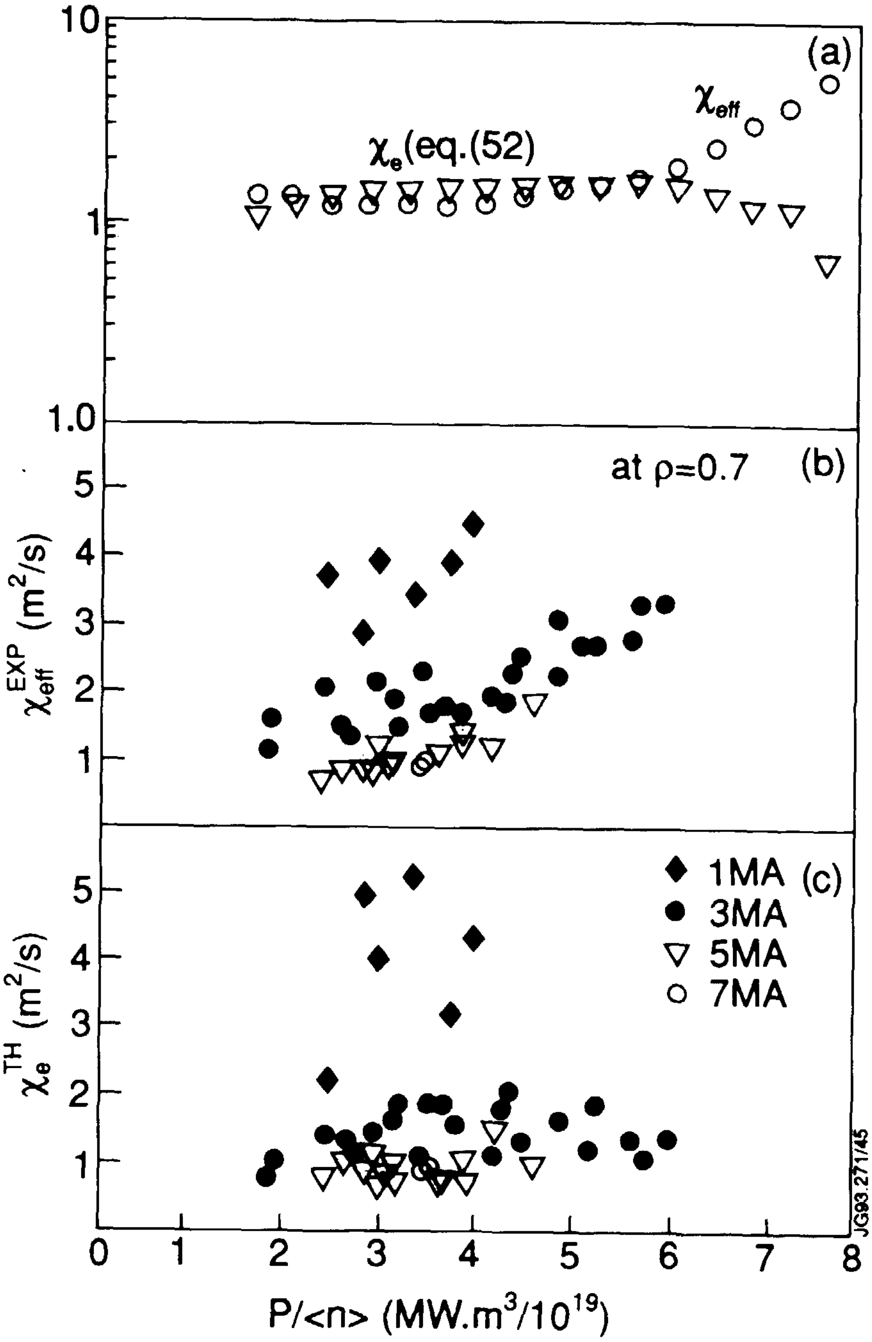

Figure 24. (a) Magnitude and radial variation of χ_e predicted by Kadomtsev's "slanted island" model in the limit of strong island overlap (Eq. (52)). The comparison between measured (b) and predicted (c) heat transport is based here on a set of JET L-mode data obtained at different current and input power levels, with average plasma density $2.0 < \langle n_e \rangle (10^{19} m^{-3}) < 3.5$.